BIOCHEMICAL AND GENETIC CHARACTERIZATION OF BACTERIOPHAGE 21 HOLIN: S^{21} AS A MEMBRANE PROTEIN AND BEYOND

A Dissertation

by

TAEHYUN PARK

Submitted to the Office of Graduate Studies of
Texas A&M University
in partial fulfillment of the requirements for the degree of

DOCTOR OF PHILOSOPHY

December 2006

Major Subject: Biochemistry

BIOCHEMICAL AND GENETIC CHARACTERIZATION OF BACTERIOPHAGE 21 HOLIN: S^{21} AS A MEMBRANE PROTEIN AND BEYOND

A Dissertation

by

TAEHYUN PARK

Submitted to the Office of Graduate Studies of
Texas A&M University
in partial fulfillment of the requirements for the degree of

DOCTOR OF PHILOSOPHY

Approved by:

Chair of Committee,	Ryland F. Young
Committee Members,	David O. Peterson
	Michael Polymenis
	Michael Benedik
Head of Department,	Gregory D. Reinhart

December 2006

Major Subject: Biochemistry

ABSTRACT

Biochemical and Genetic Characterization of Bacteriophage 21 Holin:

S^{21} as a Membrane Protein and Beyond. (December 2006)

Taehyun Park, B.S., Kyungpook National University; M.S., Minnesota State University

Chair of Advisory Committee: Dr. Ryland F. Young

The fate of phage-infected bacteria is determined by the holin, a small membrane protein that triggers disruption of the membrane at a programmed time, allowing a lysozyme to attack the cell wall. $S^{21}68$, the holin of phage 21, has two transmembrane domains (TMDs) with a predicted N-in, C-in topology. Surprisingly, TMD1 of $S^{21}68$ was found to be dispensable for function, to behave as a SAR ("signal-anchor-release") domain in exiting the membrane to the periplasm, and to engage in homotypic interactions in the soluble phase. The departure of TMD1 from the bilayer coincides with the lethal triggering of the holin and is accelerated by membrane depolarization. Basic residues added at the N-terminus of $S^{21}68$ prevent the escape of TMD1 to the periplasm and block hole formation by TMD2. Lysis thus depends on dynamic topology, in that removal of the inhibitory TMD1 from the bilayer frees TMD2 for programmed formation of lethal membrane lesions. Like the holin S of λ, the holin of lambdoid phage 21 (S^{21}) controls lysis by forming holes in the membrane. However, unlike S^{λ}, these holes are small, serving only to depolarize the membrane facilitating the release and activation of the SAR endolysin, R^{21}. We were able to demonstrate that, unlike S^{λ}, $S^{21}68$

forms a “pinhole”, thus macromolecules easily pass through S^{λ} but not S^{21} holes. This result again supports our interpretation: when S^{21} triggers, it only needs to collapse the membrane potential, thus causing release and activation of the membrane-tethered inactive SAR endolysin, but does not form holes in the membrane large enough to allow passage of a pre-folded, active cytoplasmic endolysin. The lysis defective *S^{21}68* mutant alleles were isolated throughout the *S^{21}* gene. Although the majority of lysis defective mutations occurred in the codons for the TMD2 domain, two mutations were found in the codons for the TMD1. This result suggests that only the TMD2 domain of $S^{21}68$ is likely to participate in actual hole formation. One can assume that two mutant alleles of TMD1 are involved in two different interactions: (a) TMD1-TMD1 intermolecular interaction, (b) TMD1-TMD2 intramolecular interaction. We showed that there is a specific TMD1-TMD2 interaction. In terms of TMD1-TMD2 interaction, the mutated residues of the two TMD1 mutants might prevent a departure of TMD1 from TMD2, resulting in the lysis defective phenotype. Hopefully, these findings deliver some hints about the mechanism of $S^{21}68$ hole formation and further provoke more extensive work which is required to provide a definite answer to many questions regarding this matter.

DEDICATION

This dissertation is dedicated to my dearest parents, who have believed in me even in difficult times; to my lovely wife, Hyojeong, who was there for me all these years; and to my considerate son, JoonMo and adorable daughter, Garlyne, whose love brings so much happiness to my life.

ACKNOWLEDGMENTS

I deeply acknowledge my advisor, Ryland Young. Without his support, guidance, patience, and vision this project would not have been possible. I would like to express my appreciation for my committee members, Michael Polymenis, Michael Benedik, David Peterson. I especially wish to thank Douglas Struck for his insightful discussions, patience, and moral support. I am indebted to Daisy Wilbert for clerical assistance. Special and many thanks to my past and present peers in the Young Lab: William Roof, Ing-Nang Wang, Erlan Ramanculov, Tom Bernhardt, Angelika Gründling, Liz Summer, John Deaton, Max Barenboim, Min Xu, Tram Anh Tran, Carrie Langlais, Rebecca White, Brenley McIntosh, Christos Savva, Yi Zheng, Joel Berry, Ting Pang, Gabby Kuty and Jill Dewey. I also appreciate the help of all the undergraduate student workers in the Young Lab. Without the support of these people, this dissertation would have been a much more difficult work.

TABLE OF CONTENTS

CHAPTER Page

CHAPTER Page

LIST OF FIGURES

FIGURE Page

LIST OF TABLES

CHAPTER I

INTRODUCTION

I.1. Classification of bacteriophage

The discovery of bacteriophage was made independently by two scientists in early 1900′s. The British pathologist Frederick William Twort first observed a glassy transformation of bacteria colonies, which indicates the lysis of the bacterial cells growing on solid media. Shortly thereafter, Félix Hubert d′Hérelle observed almost same phenomenon in liquid culture. Hérelle called the agent responsible for bacteria killing bacteria phage. In subsequent years, many scientists attempted to classify bacteriophages. These efforts were unsuccessful because there was no consensus as to which features of bacteriophage should serve as the basis for their subdivision. A major breakthrough occurred with the development of the electron microscope which allowed the classification of bacteriophages based on morphology in addition to their genome structure. Lwoff et al. introduced the order Urovirales for tailed phages, and families *Inoviridae* and *Microviridae* for filamentous and ϕX-type phages, respectively (Lwoff *et al.*, 1962). Following Lwoff's milestone work, a more specific system of classification was proposed by Bradley. In his system, bacteriophages are classified into six basic phage types, namely, tailed phages, filamentous phages, and icosahedral phage with single-stranded DNA (ssDNA) or single-stranded RNA (ssRNA) genome.

This dissertation follows the style and format of *Molecular Microbiology*.

The tailed phages, then, were subject to further classification resulting in contractile, long and non-contractile, or short and contractile tailed phages, In 1971, the International Committee on Taxonomy of viruses (ICTV) presented six genera based on Bradley's basic types. Representatives of each genera are T4, λ, ϕX174, MS2, fd, and PM2 (Wheeler *et al.*, 2000). Since then, additional phage groups have been identified and at present, the ICTV recognizes one order, 13 families and 31 genera of phages. (Van Regenmortel, 2000)

I.2. Bacteriophage life cycle

The life cycle of bacteriophage involves three stages. First, there is adsorption, which includes diffusion-mediated collision between phage and bacterium and the attachment of phage to their receptors. In the second stage, infection, the transfer of the phage genome to the bacterial host, occurs. This process results in what is called the eclipse period during which phage-specific proteins and nucleic acids are synthesized. From these components, phage progeny are assembled. Finally, in the third stage, the progeny are released by lysis, extrusion or budding, completing the life cycle of the bacteriophage (Abedon, 2006).

I.3. Different modes of progeny release

I.3.1. Inhibition of peptidoglycan synthesis

Escape of phage progeny from the infected host involves compromising its seemingly formidable barrier, the bacterial cell wall. The cell wall is a unique prokaryotic structure that protects bacteria from osmotic lysis and determines the shape of the cell. The cell wall is a continuous mesh of peptidoglycan. In 1973, Ozaki and Valentine proposed that ssRNA phage, Qβ, brought about host lysis by a mechanism analogous to that of antibiotics which inhibited cell wall biosynthesis (Ozaki and Valentine, 1973). Moreover, they suggested that all other small phage would use a similar mode of escape from their hosts. Direct support for this hypothesis came from the work of Bernhardt et al. who demonstrated that the lysis proteins of Qβ and ϕ174 blocked specific steps in peptidoglycan synthesis. A discussion of how these lysis proteins work is beyond a scope of this study and this mechanism of host lysis will not be considered further.

I.3.2. Peptidoglycan degradation

All dsDNA phages use a multigenic system for lysis of their hosts. In contrast to the bacterial cell wall synthesis inhibition of the small ssRNA and ssDNA phages, dsDNA phages actively degrade the cell wall of their hosts. The multigenic system consists of three proteins or protein complexes; a holin, an endolysin and a spanin. In this system, the endolysin is essential for host lysis under all conditions while the timing of lysis is under control of the holin.

I.4. Multigenic phage lysis systems: holins and endolysins

I.4.1. Holins

The holin is a small phage-encoded membrane protein. For all endolysins, lacking secretory signals, the holin is required for the endolysin to penetrate the cytoplasmic membrane (Young, 1992; Young *et al.*, 2000). In the cases where the endolysin is secreted by the *sec* system, the holin appears to cause activation of the muralytic activity by depolarizing the cytoplasmic membrane (Young *et al.*, 2000; Xu *et al.*, 2004). In either case, the key function of the holin is lysis timing: the holin is genetically programmed so that it triggers at a specific time to permeabilize the membrane (Young, 1992). Holin genes are the most diverse group with common function known in biology. There are about 250 holin genes identified, defining more than 50 unrelated orthologous gene families throughout bacteriophages of Gram negative and Gram positive bacteria (Young, 1992; Young *et al.*, 2000; Young, 2002). Most holins fall into three classes having one, two, or three transmembrane domains (TMD, Figure 1). However, some of holins are not grouped into any of three classes because of somewhat uncertain topologies based in primary sequence analysis.

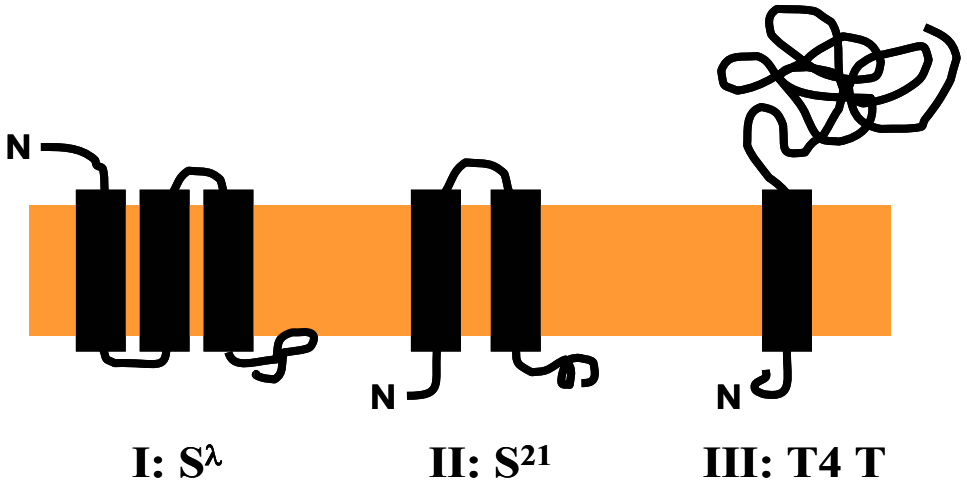

Figure 1. Membrane topology of class I, II, and III holins

I.4.2. S^{λ}, the prototype class I holin

I.4.2.1. Dual start motif of *S*

The lysis gene region of lambdoid phages has a cluster of four genes *SRRzRz1* encoding a holin, an endolysin and a heterodimeric spanin complex (Figure 2). These genes are located immediately downstream of the late gene promoter $p_{R'}$, which is turned on at about 8 min after infection by the late gene activator, Q (Garrett and Young, 1982). The *S* gene encodes two proteins by virtue of a dual start motif (Bläsi *et al.*, 1989). Each of the two start codons has its own Shine-Dalgarno sequence. Two stem-loop structures, one upstream of the coding sequence and one about 30 nucleotides into the sequence (Figure 3) control the ratio of initiations from the two start codons. Melting of the upstream stem-loop favors the initiation at the first start codon and the synthesis of a 107 residue protein, S107. By contrast, melting of the downstream stem-loop, which increases accessibility of the ribosome to the second starting codon, promotes initiation

at the second start codon, resulting in the synthesis of the shorter, S105, product. Strikingly, the S105 and S107 proteins have opposite functions. S105 is the holin for bacteriophage λ while S107 inhibits S105 function and is called an antiholin. S105 is the prototypical class I holin and has three transmembrane domains with the cytoplasmic C-terminus and the periplasmic N–terminus (Rietsch *et al.*, 1997; Gründling *et al.*, 2000a) and S105 accumulates in the cytoplasmic membrane from the beginning of late protein synthesis (about 8 minute after induction) until it is triggered. After triggering, S105 forms a lesion in the membrane which allows the R endolysin to gain access to the cell wall. The S107 protein contains two TMDs and both N- and C- terminus of 107 are cytoplasmic.

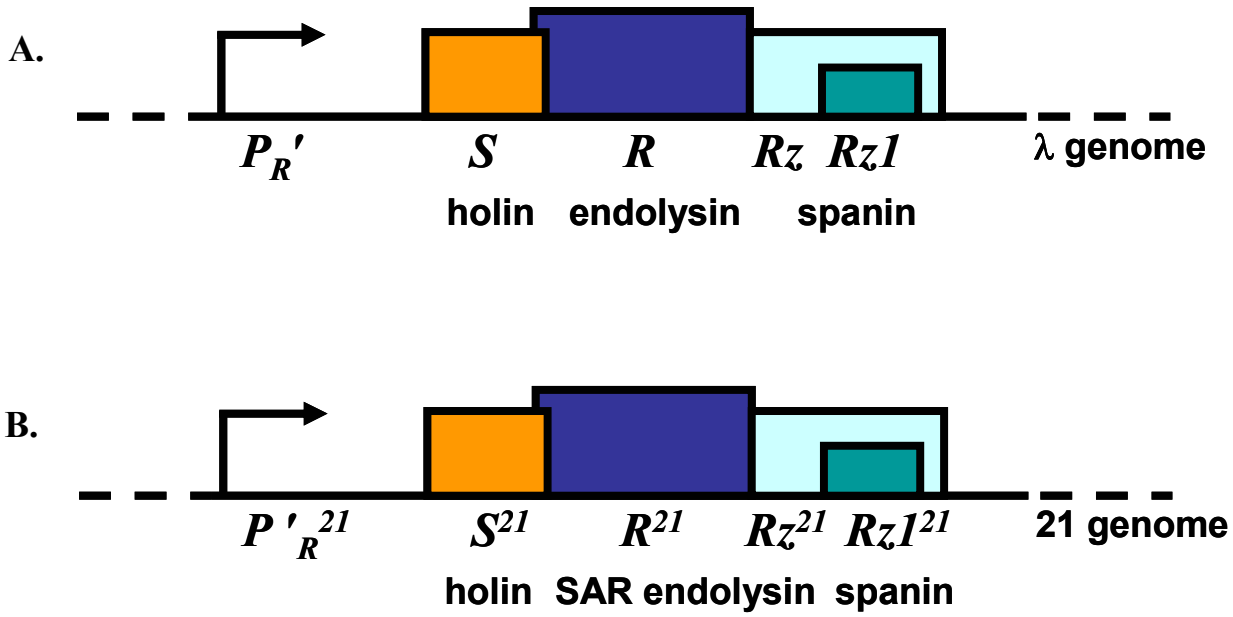

Figure 2. Lysis cassettes of lambdoid phages λ (A) and 21 (B). Note mosaicism of the lambdoid lysis cassette. The lysis genes of λ and 21 are shown, along with their late gene promoters.

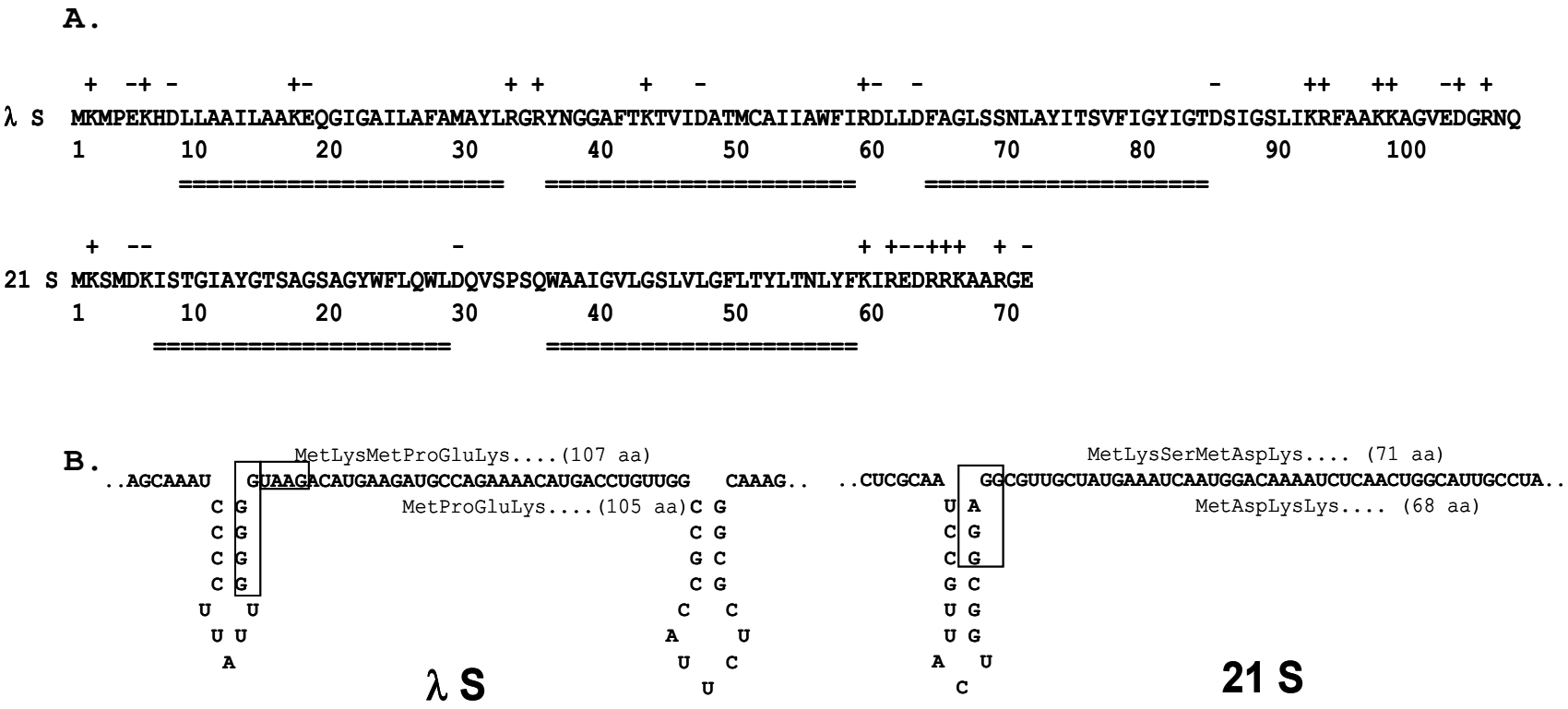

Figure 3. A. Primary sequence of S^{λ} and S^{21} holins. Charged residues are indicated above each sequence. Transmembrane domain (S^{λ}) and putative transmembrane domain (S^{21}) are marked as symbol (= =). B. Stem loop structures dictate preference of the starting Met codon for both holin and antiholin. The boxed sequences show the two Shine-Dalgarno sequences for the two translational starts of S^{λ}. In case of S^{21}, note that there is one putative stem loop structure and one Shine-Dalgarno sequence, which is supposedly used for the two translational starts of S^{21}.

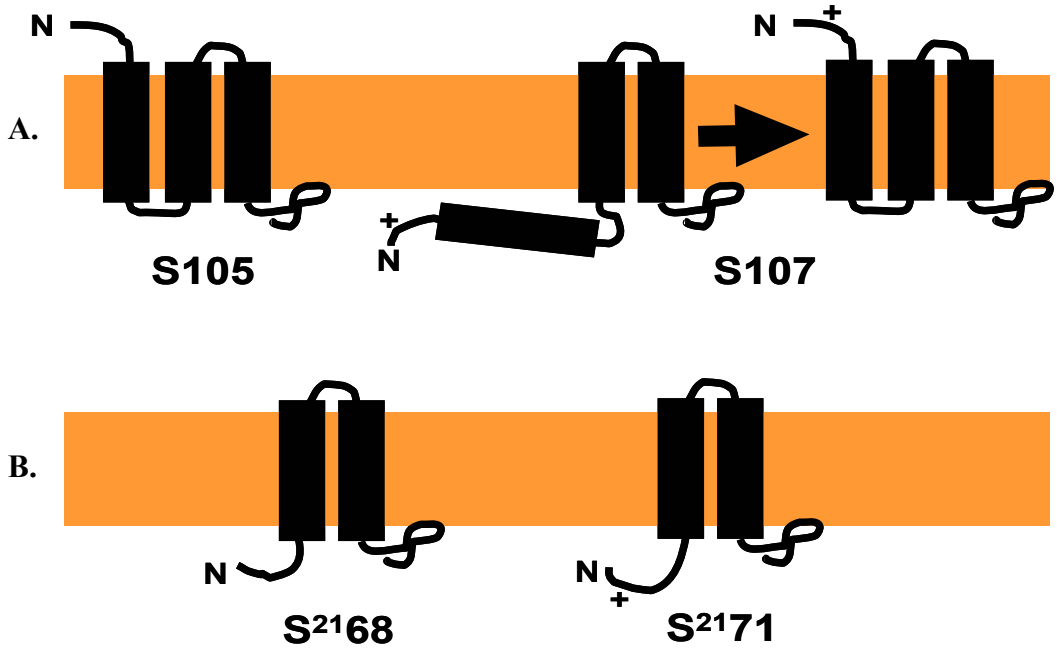

Figure 4. A. Topological change of TMD1 of Sl07 makes an "antiholin" participate as a holin in the hole formation. B. $S^{21}68$ and $S^{21}71$ presumably assume similar membrane topology. (+), positively charged residue; N, N-terminus.

Based on genetic and biochemical evidence, it was proposed that the antiholin function of S107 derives from the Lys residue at the position 2 that, when compared to S105, contributes an extra positive charge to the N-terminus. This is thought to prevent the movement of the N-terminus, including TMD1, of nascent S107 through the membrane so that the antiholin has only two TMDs (Figure 4). This form of S107 dimerizes with and inhibits S105 (Gründling *et al.*, 2000b). Normal or artificial triggering is believed to result in the movement of the N-terminus of the S107 protein across the cytoplasmic membrane forming the equivalent of the S105 TMD1 (Figure 4). Not only does this new topological isomer of S107 no longer act as an antiholin, it actually contributes to the mass of functional holin in the cytoplasmic membrane of the

infected cell (Bläsi *et al.*, 1990), presumably making lysis more rapid and efficient (Young, 2002).

At the time of host lysis, the S105:S107 ratio inside cell is about 2.5:1. When S107 is made in excess of S105, host cell lysis is blocked (Chang *et al.*, 1995; Bläsi *et al.*, 1990). When the membrane potential is collapsed, inhibition of lysis function was compromised, suggesting a model in which the N-terminal transmembrane domain of S107 is prevented from flipping through the cytoplasmic membrane by the energized membrane. The current model for antiholin function is that S107 titrates S105, by forming a hetero-dimer. This reduces the number of S105-S105 homodimers, which delays holin action. When holin is triggered at a programmed time point, the first hole is formed collapsing the membrane potential. This triggers the translocation of the N-terminal TMD of S107 across the membrane, which converts the S105-S107 heterodimer into functional holin dimers.

I.4.3. Mechanism of action of S^{λ}

Wang et al. have proposed that holins accumulate in the cytoplasmic membrane forming protein-rich regions (rafts) in which lipid is largely excluded due to close packing of their TMD (Wang *et al.*, 2003). The spontaneous formation of a defect or channel in the raft allows a localized depolarization of the cytoplasmic membrane leading to conformational changes in the bulk holin population. The end result is a rearrangement of the holin TMDs so that a large pore or channel is formed lined with the hydrophilic faces of the holin TMDs (Figure 5). This model predicts that holin function

will involve numerous interactions between the TMD helices in the same and in adjacent holin molecules. A genetic analysis of *S* was conducted to look for mutant alleles that would be useful in determining the pathway for hole-formation. It was anticipated that mapping dominant and recessive alleles might lead to identifying domains of S needed for intermolecular interactions. Lysis-defective S mutants were isolated (Raab *et al.*, 1986). Many of these S mutants were found to have defects in dimer formation or oligomer formation. A few had a normal pattern of oligomerization despite the loss of lytic function. The simplest interpretation of these mutants is that the pathway for lysis starts with the formation of dimers, followed by higher order oligomerization and then a concerted conformational change which leads to lesion-formation (Figure 5). Some lysis-defective alleles cause a substantial delay in lysis in the presence of the wt S allele and are considered to have dominant character. Surprisingly, a few lysis-defective S alleles cause lysis even earlier than double wild type when paired with S+. This phenotype is named "anti-dominance"(Raab *et al.*, 1988). The anti-dominance phenotype seems to derive from interactions, between S mutant and S wild-type protein, which affect the timing function intrinsic to the S sequence. This result indicates an important aspect of the S protein. That is, there are direct interactions between holin molecules, such as oligomerization.

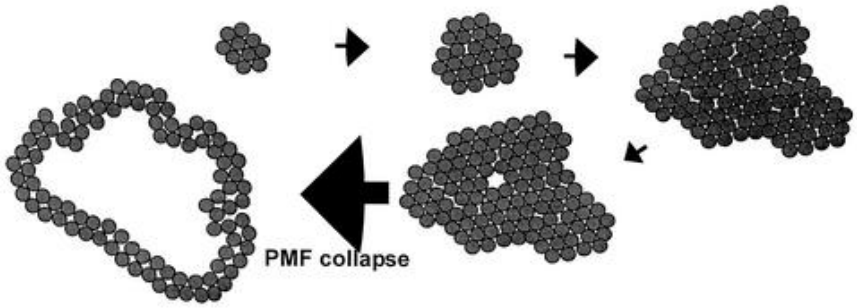

Figure 5. Current model for the formation of a holin lesion. (A) Holin rafts. Holins accumulate in rafts in the membrane. In the rafts, holins are tightly positioned against each other by intimate helix packing via TMDs, resulting in excluding lipids. Spontaneous formation of an aqueous channel by thermal fluctuation is described. The localized depolarization causes a conformational change in the holins, leading to asymmetric disruption of the helix packing, exposure of a relatively hydrophilic surface, and dispersion of the subunits into the holin lesion. Each circle represents a single holin molecule. PMF, proton motive force (adopted from (Wang *et al.*, 2003).

In a separate approach, an in vitro system to study S function has been developed. Purified his-tagged S protein has been shown to permeabilize liposomes while the lysis-defective holin, A52V, is inactive in these assays (Figure 6). The simplest interpretation is that S itself is necessary and sufficient to make a permeabilizing lesion. This system might be useful to dissect the structure of the holin complexes which allow passage of macromolecules across the cytoplasmic membrane.

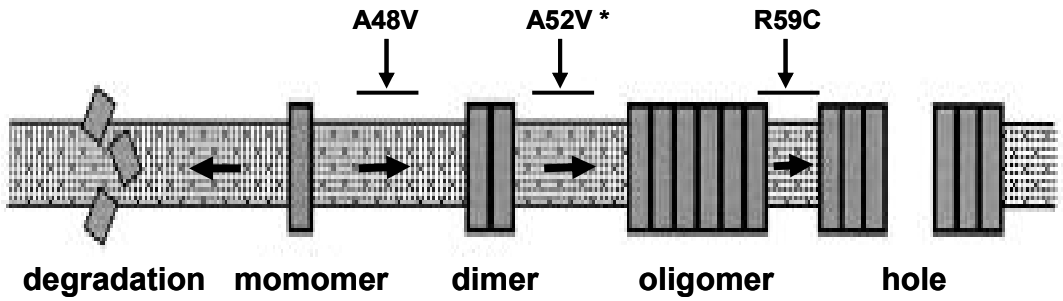

Figure 6. Model for hole formation. The S molecule was depicted as a gray rectangle for simplicity purpose. Three steps are required for hole formation at least. The steps are: monomerization, dimerization, and oligomerization, thus, leading into hole formation. The mutant alleles corresponding to each step were indicated. A symbol (*) indicates a representative of the dimerization defective alleles .

I.4.4. S^{21}, the prototype class II holin

The lysis gene region of lambdoid bacteriophage 21 is a cluster of four genes, SRRzRz1. The S protein from the lambdoid bacteriophage 21, S^{21}, is the prototype of class II holins (Figure 2). Class II holins are smaller (60-85 residues) than the class I holins and have only two predicted transmembrane helices (Smith *et al.*, 1998; Bonovich and Young, 1991; Barenboim *et al.*, 1999; Young and Bläsi, 1995). Like most holin genes of lambdoid phages, the *S* gene of phage 21 has a "dual-start motif" that controls the ratio between S^{21}68 (holin) and S^{21}71 (holin-inhibitor) (Bläsi *et al.*, 1989; Young and Bläsi, 1995; Bläsi *et al.*, 1990). S^{21}71 is identical to S^{21}68 except for the N-terminal sequence Met-Lys-Ser..., which provides an additional positive charge when compared to the N-terminus of S^{21}68. Compared to S^{λ}, relatively little is known about S^{21}. In

particular, it has not been subjected to a thorough genetic analysis. It is not known where lysis timing mutants can occur, or whether either putative TMD is important for "hole-formation". No missense mutants have been isolated, which handicaps biochemical analysis of S^{21}. It is not known whether S^{21} can be altered to function with endolysin lacking signal sequence domain (i.e. whether S^{21} "holes" can be made permissive for R^{λ} by mutation.). Also, a possible topological change of S^{21} upon hole formation, in analogy with S^{λ}, has never been studied.

I.4.5. T4 T, the prototype class III holin

Bacteriophage T4 T is the only known type III holin. It is 218 amino acids in length and is highly hydrophilic. Although it is considerably larger than either type I or type II holins, T4 T contains only one transmembrane domain with N-terminus in and C-terminus out topology. Its most distinctive feature is a large C-terminal periplasmic domain of 163 residues. Unlike the *S* genes of phage λ and phage 21, the T4 *t* gene encodes a single protein. The antiholin for T4 is encoded by a separate gene, *rI* which encodes a protein with a single transmembrane domain flanked by a short N-terminal extension located in the cytoplasm and a larger C-terminal periplasmic domain. In the late 1940′s, it was reported that cells infected with T4 at high multiplicities displayed a phenotype called lysis inhibition (LIN) where the lysis of the infected cells is delayed due to secondary infections by T4 (Doermann, 1948; Hershey, 1946). In *E. coli* K-12 strains, the *rI* gene is necessary and sufficient for the establishment of LIN in cells expressing the T4 *t* gene. The T and RI proteins have been shown to interact with each

other by chemical crosslinking (Ramanculov and Young, 2001) and co-immunoprecipitation (Tran *et al.*, 2005). This interaction occurs between the periplasmic domains of these two proteins.

I.4.6. Phage-encoded endolysins

Completion of the bacteriophage lytic cycle requires lysis of their bacterial host. Phage with a double-stranded DNA genome lyses host cells by a holin-endolysin system (Young, 2002; Young, 1992; Young *et al.*, 2000). The endolysin, a muralytic enzyme, degrades the peptidoglycan. The endolysins from double-stranded DNA phage are functionally classified into at least four different kinds of enzymes: (a) R^{λ} and P2 K transglycosylases which hydrolyze β(1,4)-glycosidic bonds, but maintain the bond energy by forming the cyclic 1,6-disccharide product (Bienkowska-Szewczyk *et al.*, 1981), (b) the P22 gp19 (Rennell and Poteete, 1985) and T4 E lysozymes (Tsugita and Inouye, 1968a), which also cleave glycosidic bond, but do not conserve the bond energy, (c) the A500 ply500 endopeptidase (Loessner *et al.*, 1995), which cleaves between amino acid residues, and the T7 gp3.5 amidase (Inouye *et al.*, 1973), which cleaves the amide bond between aminoglycosidic subunits and tetrapeptide chains (Figure 7). The crystal structures of R^{λ} (Evrard *et al.*, 1998), T7 gp3.5 (Cheng *et al.*, 1994), and T4 E (Weaver and Matthews, 1987), have been solved and it appeared that they do not share any common structural features other than they are about 20 kDa in molecular mass and have monomeric and globular status. Until recently, it was thought that a common feature of endolysins was the lack of a secretory signal. Thus the endolysins seemed to

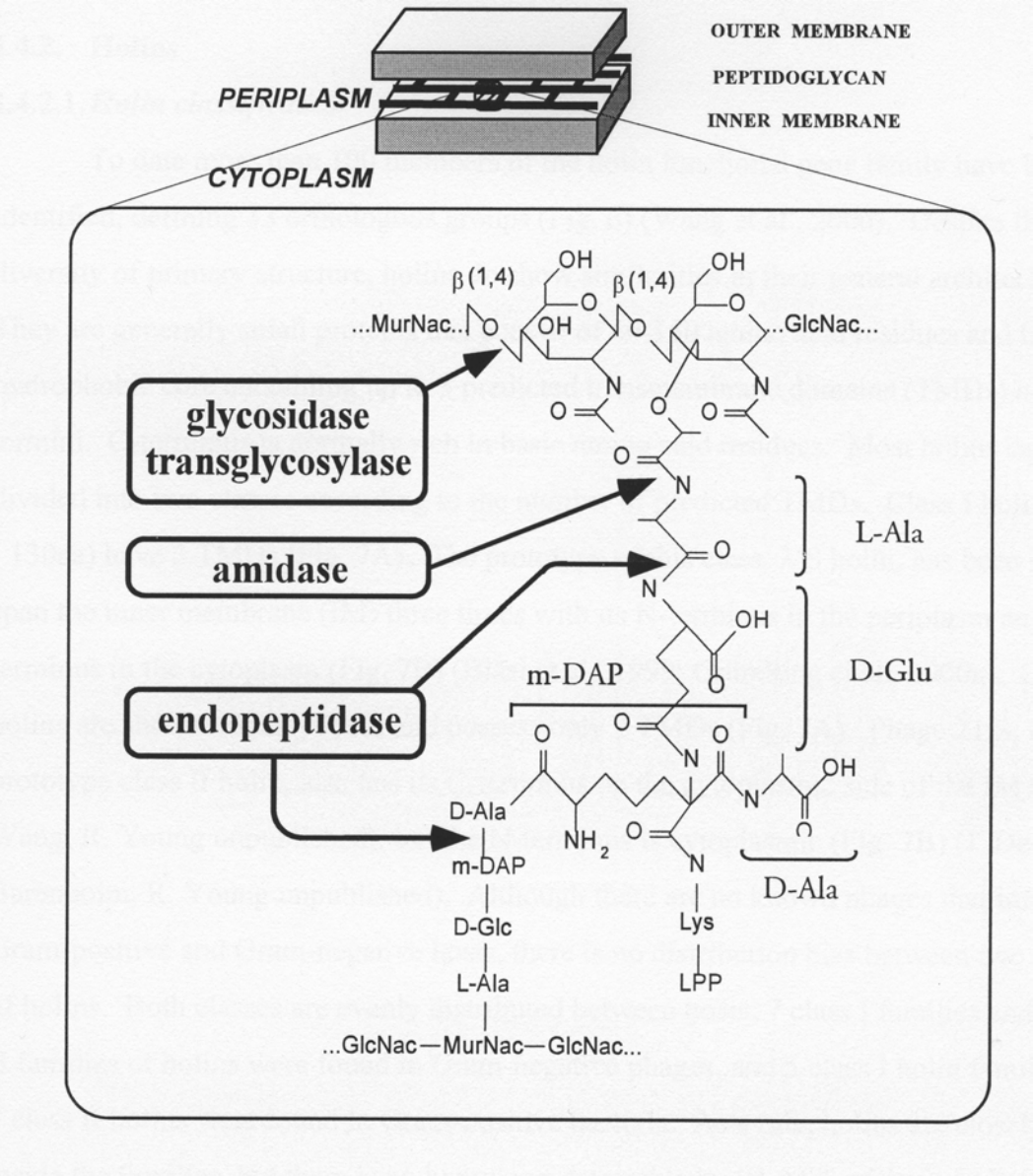

Figure 7. A schematic drawing of Gram-negative bacterial peptidoglycan structure and sites of cleavage by various endolysins. Abbreviations: GlcNac, N-acetylglucosamine; MurNac, N-acetylmuramic acid; L/D-Ala, L/D alanine; D-Glu, D-glutamic acid; m-DAP, meso-diaminopimelic acid; Lys, lysine; LPP, Braun's lipoprotein. (Adopted from Ramanculov's dissertation).

require another protein for access to the cell wall. Recently, endolysins containing an N-terminal signal sequence have been reported. However, even in these cases, the phage has a holin gene (Sao-Jose *et al.*, 2000).

I.4.6.1. Cytoplasmic endolysin

T4 E is a cytoplasmic "true lysozyme." It is small (164 aa long), basic (pI 9.6), soluble globular monomeric protein, which are common characteristics of phage endolysin (Weaver and Matthews, 1987). Its peptidoglycan degrading activity is well studied. (Streisinger *et al.*, 1961; Tsugita and Inouye, 1968b). It was demonstrated that gene *e* functions efficiently with *S* gene of λ. R^{λ}, the endolysin, is a soluble transglycosylase. The endolysin accumulates fully folded in the cytoplasm until the S holins accumulating in the host membrane are triggered to form "holes"(Chang *et al.*, 1993; Chang *et al.*, 1995). Until an access to the cell wall is provided by hole formation, the accumulation of either R^{λ} or T4 E does not affect integrity of the cell wall.

I.4.6.2. Endolysins with SAR domain

The Lyz protein, the endolysin of bacteriophage P1, is 185 aa long and is homologous to the T4 E lysozyme. The Lyz protein is a prototype of SAR endolysin (Xu *et al.*, 2004). The SAR endolysin contains a signal-arrest-release (SAR) domain which is very rich in non-hydrophobic amino acid residues such as Ala, Gly, Ser, and Thr. The signal sequence domain of P1 Lyz is not cleaved after insertion into the membrane by host *sec* system. Common characteristics of SAR endolysin are: (a) SAR endolysins

cause host lysis in the absence of holin, (b) SAR endolysins are exported by *sec* system which recognizes their N-terminal SAR domain, (c) The SAR domain allows release of SAR endolysin from the membrane. The endolysins from several other phages of Gram negative bacteria are predicted to share this feature. (Figure 8).

The phage 21 endolysin, R^{21}, is 165 amino acid long and it is a muraminidase or classic "true lysozyme" based on its sequence similarity to P22 19 (34% identity) and the prototype E lysozyme of T4. Recently, it has been discovered that R^{21} contains a SAR domain similar to that of P1 Lyz (Xu *et al.*, 2004). As with P1 lyz, R^{21} can cause host lysis independent of holin shown in the same study above.

This discovery gives rise to an important question: if R^{21} externalized without the help of holin, what is the role of the holin?

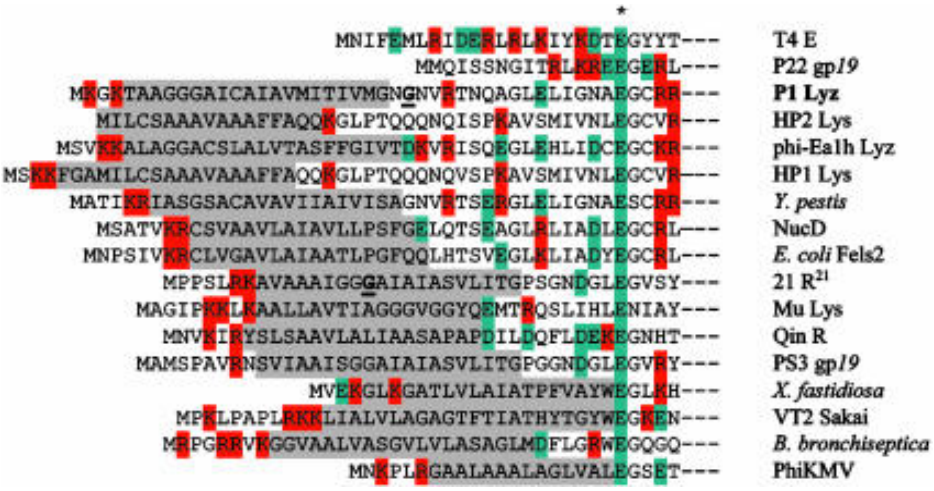

Figure 8. Alignment of N-terminal sequences of P1 Lyz and other homologs of T4 E lysozyme. A symbol (*) indicates the presumptive catalytic Glu residue. The putative SAR domains are highlighted as in gray, and basic and acidic residues are highlighted in res and green, respectively. (Adopted from (Xu *et al.*, 2004).

I.4.7. Spanin

I.4.7.1. Two component spanin: Rz and Rz1

Since Jacob and Fuerst showed that a bacteriolytic enzyme (λ endolysin) exists in the induced culture of an E. coli lysogen (Jacob and Fuerst, 1958), a series of attempts to purify phage endolysin were conducted. As results, phage endolysin had been partially or completely purified by two different groups (Work, 1967; Black and Hogness, 1969). An activity of fore-mentioned phage endolysin was ascribed to endopeptidase, which has a different mode of activity when it is compared to lysozyme, a term exclusively used for muramidases of egg white (Taylor, 1971). Since the discovery of the *Rz* gene in the λ genome (Young *et al.*, 1979), the search for *Rz*-like genes was performed. Because of a surprising similarity in gene arrangement, bacteriophage P22 was first scrutinized and found to contain an *Rz*-like gene, *19*, within a lysis gene cassette, along with T7 *18.5* gene. Both P22 *19* and T7 *18.5* genes showed extensive amino acid sequence similarity and weak similarity, respectively (Casjens *et al.*, 1989). One interesting and unexpected discovery was made by Hanych et. al. (Hanych *et al.*, 1993). When they expressed a cloned *Rz* gene, they found two protein bands of 6.5 kDa and 17.2 kDa. Base on a deduced molecular weight from the DNA sequence of *Rz* and a complementation experiment, the 17.2 kDa protein was ascribed to *Rz* gene. In the case of lambda, the *Rz1* coding region is totally embedded in the*Rz* in a +1 reading frame (Zhang and Young, 1999). Sequence analysis of *Rz* and *Rz1* indicates that they are a periplasmic protein and an outer-membrane lipoprotein, respectively. Notably, *Rz*-like gene has yet to be found in Gram positive bacteria. It has been

established that both of these auxiliary lysis genes are required for host cell lysis if the outer membrane is stabilized by more than 10 mM of divalent cations. The function of Rz and Rz1 is unknown; however it has been speculated that their role in cell lysis is to cleave oligopeptide links between the murein cell wall and outer membrane lipoproteins (Young *et al.*, 2000).

I.4.7.2. One component spanin: spanin

Recently, one component spanin was discovered in bacteriophage T1 (Summer, 2006). The gene *11*, which is located in the lysis cassette of the T1 phage, encodes a spanin. The gp11 is 132 aa in length and is an outer membrane lipoprotein with C-terminal TMDs and thus, it is believed, to span the periplasm. It is expected that many members of Gram negative phages might carry spanin genes.

I.5. Objectives

I.5.1. What distinguishes $S^{21}68$ and $S^{21}71$?

As previously mentioned, both $S^{21}68$ and $S^{21}71$ proteins have two transmembrane domains and N-in, C-in topology. Interestingly, the only noticeable difference between the two proteins is that $S^{21}71$ contains one extra positive charge at the N-terminus. One major question asked in this study is "what makes $S^{21}68$ and $S^{21}71$ different from one another?" Our original hypothesis was that there has to be some form of topological changes in S^{21} proteins. Originating from that simple hypothesis, interesting and unprecedented new results have been obtained and described in detail in

the following chapter.

I.5.2. Are large holes necessary if a SAR endolysin is used ?

In the previous section it was mentioned that R^{21} can cause host lysis independent of holin. Based on this discovery we ask, if R^{21} externalized without the help of holin, what is the role of the holin?

I.5.3. Conduct a saturating mutational analysis of the S^{21} holin gene for missense mutants

Isolation of lysis defective mutants: λ holin has been demonstrated to contain an intrinsic clock which is affected by a single missense amino acid change in its sequence as shown in bacteriophage λ (Bläsi *et al.*, 1989; Young and Bläsi, 1995; Bläsi *et al.*, 1990; Raab *et al.*, 1986). The saturating mutational analysis of the S^{21} holin gene can provide information about two important questions: (a) residues important for the function of the intrinsic clock and (b) the particular steps involved in lysis. Mutation of the residues important for the intrinsic clock will affect lysis timing, which can be observed through lysis curves. Information obtained from the mutational analysis of S^{21} can also be used to correlate the lysis defects with defects at the molecular level using cross-linking. In order to achieve this goal, a genetic selection system for $S^{21}68$ mutant alleles was developed. At least four different types of $S^{21}68$ mutants are expected from the mutational analysis: lysis timing, lysis defect, dominant and recessive mutants. The lysis timing mutants of $S^{21}68$ will cause changes in lysis timing, while the lysis defect

mutants will abolish lysis function of $S^{21}68$. Dominant and recessive aspects of the $S^{21}68$ mutants will not be discussed in this study.

CHAPTER II

TOPOLOGICAL DYNAMICS OF HOLINS IN PROGRAMMED BACTERIAL LYSIS *

II.1. Introduction

Much of the world's biomass is turned over daily in ~10^{28} phage infections of bacterial cells (Fuhrman, 1999; Hendrix *et al.*, 1999). For most phages, each infection cycle terminates with the strictly programmed and regulated lysis of the host brought about by two phage-encoded proteins, the endolysin, or lysozyme, and the holin, a small membrane protein that controls lysozyme function (Young *et al.*, 2000; Young, 1992). During phage assembly, holin molecules accumulate in the cytoplasmic membrane without detectable effect on the host (Gründling *et al.*, 2001; Wang *et al.*, 2000). Then, at a time programmed into their primary structure, holins trigger to disrupt the cytoplasmic membrane. For phages like λ and T4, this allows release of an active lysozyme that has accumulated in the cytosol, and holin function is absolutely required for lysis. For others, like P1 and the lambdoid phage 21, the lysozyme is exported by the host *sec* system and accumulates in the periplasm as an enzymatically inactive form tethered to the membrane by an N-terminal SAR ("signal anchor-release") sequence (Xu *et al.*, 2004; Xu *et al.*, 2005). Unlike canonical transmembrane domains (TMDs), SAR domains have the unique property of escaping from the bilayer, in part because of an

---

* Reprinted from Park, T., Struck, D.K., Deaton, J.F., Young, R. (2007) Topological dynamics of holins in programmed bacterial lysis. *Proc Natl Acad Sci USA* accepted.

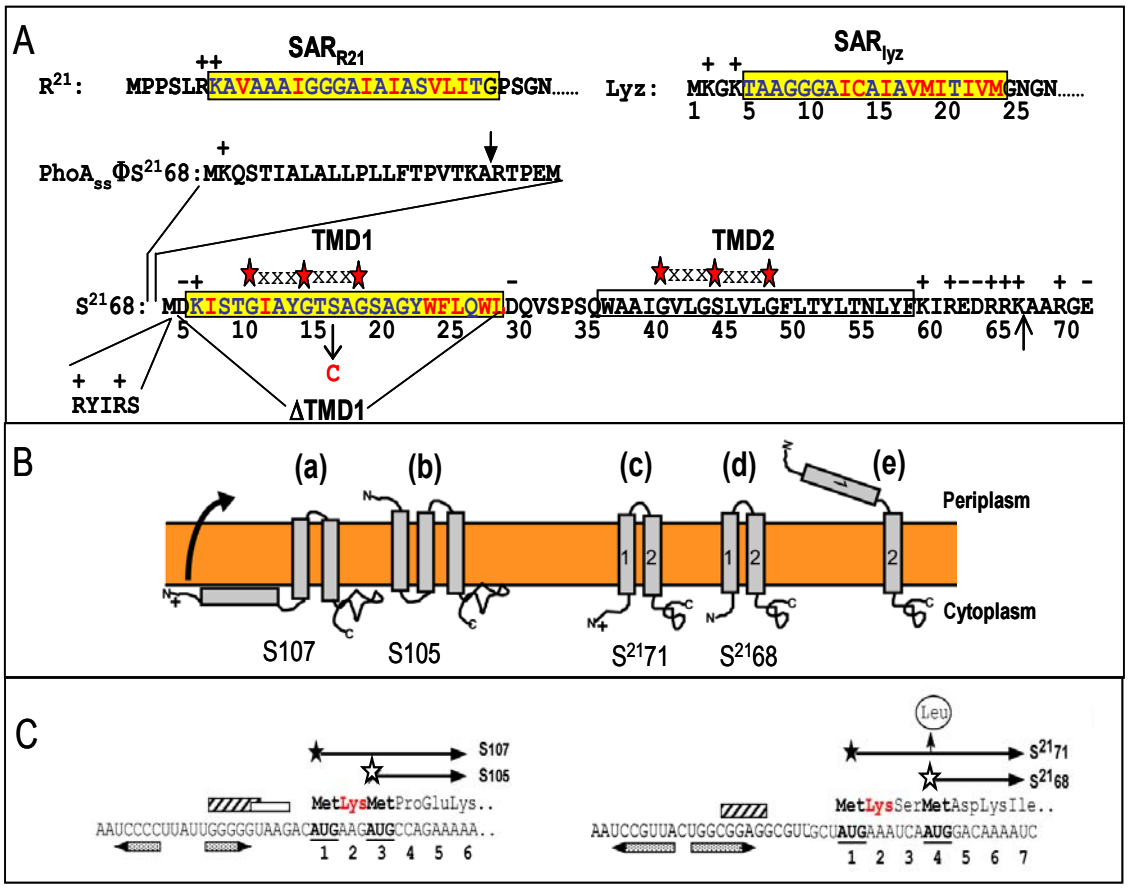

Figure 9. Properties of holins and holin genes. (A) Primary structure of $S^{21}68$ and the N-terminal domains of Lyz, R^{21}, and PhoA. The codon numbering for $S^{21}68$ follows that of the full length gene product, $S^{21}71$ (see panel C for the dual-start structure at the beginning of S^{21}). The SAR sequences of Lyz and R^{21} (Xu *et al.*, 2005; Xu *et al.*, 2004) and TMD1 of $S^{21}68$ (Bonovich and Young, 1991) are shown in the yellow boxes, with the residues that are polar or neutral in terms of hydrophobicity in blue and the hydrophobic residues in red. TMD2 of $S^{21}68$ is shown in an uncolored box. The red stars separated by three X's above the TMDs of S^{21} indicate GxxxG-like motifs that may mediate interhelical interactions (Senes *et al.*, 2004). The vertical arrow above the PhoA sequence indicates the normal signal sequence cleavage site (Inouye *et al.*, 1982). In ^{ss}PhoA$\Phi S^{21}68$, the bracketed sequence from PhoA is fused to the Met_4 codon of S^{21}. The position of the S16C missense change is indicated by a vertical arrow below the TMD1 sequence. The N-terminus of $S^{21}68$ was given two additional positive charges by inserting the sequence RYIRS between positions 4 and 5. To generate $S^{21}68_{\Delta TMD1}$, the bracketed sequence was deleted from $S^{21}68$. The vertical arrow between residues 66 and 67 indicates the position where the sequence $G_2H_6G_2$ was inserted in the allele used for purification. (B) Holin topologies. The topologies of the λ antiholin, S107 (a), and holin, S105 (b), are shown (Graschopf and Bläsi, 1999a; Graschopf and Bläsi, 1999b; Gründling *et al.*, 2000a; Wang *et al.*, 2000). (c) and (d) show $S^{21}71$ and $S^{21}68$ with two TMDs, respectively. In (e), the lethal form of S^{21} is shown with its TMD1 in the periplasm. (C) Translational control region of the λ and 21 holin genes (Bläsi *et al.*, 1989; Bonovich and Young, 1991; Barenboim *et al.*, 1999). Filled and empty stars show starts of the long (antiholin) and short (holin) gene products. Shine-Dalgarno sequences for the first and second translational starts of S^{λ} are indicated by striped and empty boxes, respectively. The single Shine-Dalgarno sequence of S^{21} is indicated by a striped box. The horizontal inverted pairs of arrows show the RNA stem loops controlling the dual starts. For S21, the vertical arrow shows the Met4 →Leu mutation, which eliminates the production of the holin from the allele referred to as $S^{21}71$. The Lys residues conferring antiholin character to the longer translational product in both the S and S^{21} genes are shown in red.

elevated content of relatively non-hydrophobic residues like Gly, Ala, Ser and Thr (Figure 9A). Activation of SAR lysozymes requires their release from the bilayer (Xu *et al.*, 2005). In these cases, holins are not essential for lysis but are thought to impose timing on the lytic event, because holin triggering depolarizes the membrane, and depolarization accelerates the release of the SAR lysozyme from the bilayer (Xu *et al.*, 2004).

Holins are extremely diverse but can be grouped into three classes based on their known or predicted membrane topology (Young, 2002; Wang *et al.*, 2000). The two major classes are class I, with three transmembrane domains (TMDs), and class II, with two TMDs (Figure 9B). Many of the genes for class I and class II holins encode two proteins. For example, the coding sequence of the λ *S* gene begins with codons specifying Met-Lys-Met- (Figure 9C). Both Met codons are used for translational initiation, giving rise to two proteins, S107 and S105, named for their length in amino acid residues (Raab *et al.*, 1988; Bläsi *et al.*, 1989; Bläsi *et al.*, 1990; Wang *et al.*, 2000). These two proteins differ only at their N-termini, where S107 has a Met-Lys extension with respect to S105. This small difference has a profound effect on the function of the two proteins; S105 is the holin for phage λ, whereas S107 inhibits membrane disruption by S105 and was the first protein to be designated as an "antiholin" (Young *et al.*, 2000; Wang *et al.*, 2000). Based on genetic evidence, it was proposed that the antiholin function of S107 derives from the Lys_2 residue that, when compared to S105, contributes an extra positive charge to the N-terminus. Physiological and biochemical studies indicated that this prevents movement of the N-terminus, including TMD1, of nascent

S107 through the membrane, so that the antiholin has only two TMDs (Figure 9B) (Graschopf and Bläsi, 1999b). This form of S107 dimerizes with and inhibits S105 (Gründling *et al.*, 2000c). Normal or artificial triggering is believed to result in the movement of the N-terminus of the S107 protein across the cytoplasmic membrane forming the equivalent of the S105 TMD1 (Figure 9B). Not only does this new topological isomer of S107 no longer act as an antiholin, it actually contributes to the mass of functional holin in the cytoplasmic membrane of the infected cell (Bläsi *et al.*, 1990), presumably making lysis more rapid and efficient (Young, 2002).

Like λ *S*, the holin gene of phage 21 also has a dual start and encodes two proteins, a holin, $S^{21}68$, and an antiholin, $S^{21}71$ (Figure 9C) (Barenboim *et al.*, 1999; Bonovich and Young, 1991). Here we report unexpected and unprecedented topological changes integral to the function and regulation of this class II holin.

II.2. Materials and methods

II.2.1. Bacterial strains and culture conditions

All bacterial cultures were grown in standard LB medium, supplemented with various antibiotics when appropriate: ampicillin, 100 μg/ml; chloramphenicol, 10 μg/ml; kanamycin, 40μg/ml; and tetracycline, 10 μg/ml. When indicated, isopropyl β-D-thiogalactoside (IPTG), dinitrophenol (DNP) or $CHCl_3$ were added at final concentration of 1mM, 2 mM or 1%, respectively.

Standard conditions for the growth of cultures and the monitoring of lysis kinetics have been described (Chang *et al.*, 1995; Smith *et al.*, 1998b). All experiments

were done with a *lacI*^{q1} *tonA::*Tn*10* derivative of MG1655, the sequenced wild-type strain of *E. coli* K-12 (Guyer *et al.*, 1981).

II.2.2. Standard DNA manipulation, PCR, and DNA sequencing

Procedures for the isolation of plasmid DNA, DNA amplification by PCR, PCR product purification, DNA transformation, and DNA sequencing have been described (Smith *et al.*, 1998a; Smith and Young, 1998; Gründling *et al.*, 2000a). Oligonucleotides were obtained from Integrated DNA Technologies, Coralville, IA, and were used without further purification. Ligation reactions were performed by using the Rapid DNA ligation kit from Roche Molecular Biochemicals according to the manufacturer's instructions. All other enzymes were purchased from Promega, with the exception of *Pfu* polymerase, which was from Stratagene. Automated fluorescent sequencing was performed at the Laboratory for Plant Genomic Technologies in the Crop Biotechnology Center at Texas A&M University.

II.2.3. Plasmids and induction

All experiments were done with a *lacI*^{q1} *tonA::*Tn*10* derivative of MG1655, the sequenced wild-type strain of *E. coli* K-12 (Guyer *et al.*, 1981). For most experiments, the bacterial strains carried two plasmids, a low copy plasmid pQ, carrying the gene for the λ late gene activator, Q, under $P_{lac/ara-1}$ control , and a medium copy plasmid with a pBR322 origin and the lysis gene cassette, *SRRzRz1*, under the control of the late promoter, pR' (Gründling *et al.*, 2000c). The lysis gene cassettes were either from λ or

phage 21, as indicated. Induction of the lysis genes was accomplished by adding 1 mM IPTG to the culture. In experiments where the wt or modified alleles of P1 *lyz* were induced, the only plasmid present was a derivative of pJF118, a medium copy plasmid carrying the *lyz* allele under control of the *tac* promoter (Xu *et al.*, 2004). The various S^{21} genes used in this study were expressed in constructs based on the plasmid pS105 (Gründling *et al.*, 2000b), which is a pBR322 derivative carrying the λ late promoter, $p_{R'}$, and the entire λ lysis cassette, *SRRzRz1*, on an EcoRI-ClaI fragment. The promoter is activated when the pR' activator Q is supplied from the IPTG induction of pQ. The plasmid pQ is a low copy vector with *Q* under a *lac-ara* promoter (Gründling *et al.*, 2001). The source of phage 21 lysis genes was the plasmid pBP71 (Barenboim *et al.*, 1999), which has an EcoRI-ClaI fragment carrying the genes $S^{21}71R^{21}Rz^{21}Rz1^{21}$. $S^{21}71$ is an allele of the holin gene S^{21} in which the Met_4 codon has been changed to Leu (CUG) so that only the $S^{21}71$ antiholin gene product is expressed (Figure 9C). To construct pTP1, the EcoRI-ClaI fragment in pS105 was replaced by the corresponding EcoRI-ClaI fragment from pBP71. The expression level of the $S^{21}71$ gene was increased by changing the Shine-Dalgarno sequence from cggaggc to aggaggt (positions -13 to -7 upstream of the S^{21} start codon), using site-directed mutagenesis. The plasmid pTP2, carrying the genes $S^{21}68R^{21}Rz^{21}Rz1^{21}$, has an identical structure except that the first three codons of the S^{21} gene are deleted. The sole S^{21} gene product from this allele is $S^{21}68$ (Figure 9C). The spacing between the modified Shine-Dalgarno sequence and the start codon of the S^{21} reading frame is identical for both plasmids. Missense and nonsense changes in the S^{21} and R^{21} genes of pTP1, pTP2, and others were introduced by

conventional site-directed mutagenesis using the QuikChange kit from Stratagene. To make the plasmid pTP3, codon 46 of *S*^{21}*68* in pTP2 was changed to the amber codon UAG. To make pTP4, codons 39 and 42 of *R*^{21} in pTP2 were changed to amber codons.

The first step in constructing plasmid pTP5, encoding $SAR_{lyz}\Phi S^{21}68_{\Delta TMD1}$, was amplifying the sequence encoding MKGKTAAGGGAICAIAVMITIVM from *lyz* using a upstream primer that had, at its 5' end, homology to positions -21 to -1 and a downstream primer that had, at its 5' end, homology to positions +93 to +73 of the *S*^{21}*68* gene of pTP2. The purified PCR product was used to prime a site-directed mutagenesis reaction using pTP2 as its template. In a similar fashion, the following plasmids were constructed using pTP2, pTP5 or pJFLyz as the template for the final PCR reaction, as appropriate: pTP6, encoding $^{ss}PhoA\Phi S^{21}68$, with the signal sequence (residues 1-26) of PhoA replacing the N-terminal Met of $S^{21}68$; pTP7, encoding $RYIRS\Phi S^{21}68$, with the amino acid sequence RYIRS inserted after the N-terminal Met residue of $S^{21}68$; pTP8, encoding $S^{21}68_{TMD1}\Phi Lyz_{\Delta SAR}$, with the SAR domain of Lyz replaced by TMD1 of $S^{21}68$; and pTP9, encoding $RYIRS\text{-}SAR_{lyz}\Phi S^{21}68_{\Delta TMD1}$, with the amino acid sequence RYIRS inserted after N-terminal Met residue of SAR_{lyz}. Construction of pJFLyz, pJFFtsI, pJFPhoA, and pR$^{\lambda}$, in which *lyz*, *ftsI*, *phoA*, and *R*$^{\lambda}$ are under *tac* promoter control, respectively, was previously described (Xu *et al.*, 2004). Nucleotide sequences encoding c-myc tag were introduced to *ftsI* gene by site-directed mutagenesis to construct pJFFtsIcmyc.

The construction of the plasmid $pETS^{21}68^{his}$ was carried out as previously described (Smith *et al.*, 1998b) with minor modifications. Briefly, the coding sequence

of $S^{21}68$ was amplified by PCR with NdeI and HindIII sites at its 5' and 3' end, respectively. Both purified PCR products and the pET11a vector (Novagen, San Diego, CA) were cut with NdeI and HindIII and ligated by using T4 DNA ligase (New England Biolabs, Beverly, MA). To make $pETS^{21}68^{his}$, a nucleotide sequence encoding the residues GGH_6GG was inserted between codons 66 and 67 of the *S*^{21} gene by site-directed mutagenesis.

All constructs were verified by DNA sequencing.

II.2.4. Subcellular fractionation

Subcellular fractionation has been described (Xu *et al.*, 2004). As controls, R^{λ}, the endolysin encoded by bacteriophage λ, was used for the soluble and spheroplast fraction, $FtsI^{cmyc}$ was used for the membrane fraction, and PhoA was used for the periplasmic fraction (Figures 10 and 11). In general, control samples were prepared in parallel to the experimental samples.

II.2.5. Protein expression in spheroplasts and proteinase K digestion

Spheroplasts carrying the indicated plasmids were suspended in 0.5X LB medium containing 12.5% sucrose, induced with 1mM IPTG and 0.2% arabinose, and incubated without shaking for 25 min at 37°C. Aliquots (1.5 ml) containing approximately 4 x 10^8 spheroplasts were treated with proteinase K (20 μg/ml final concentration) for the indicated times at room temperature. Proteinase K treatments were stopped by adding trichloroacetic acid (TCA), as described below.

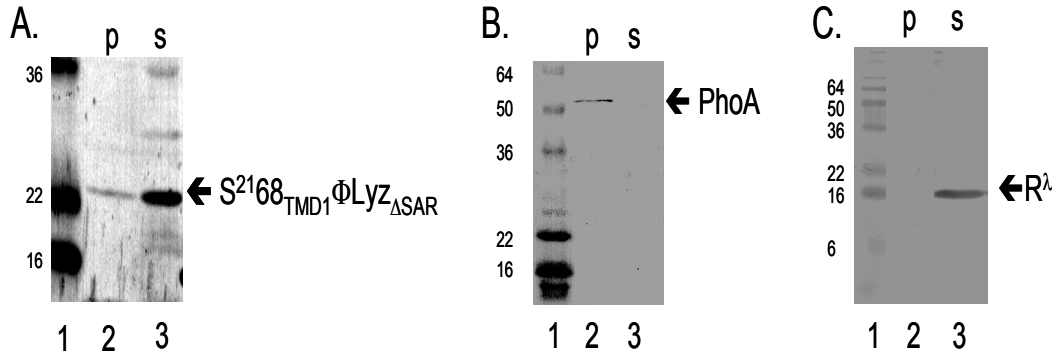

Figure 10. TMD1 of $S^{21}68$ facilitates release of P1 Lyz to the periplasm. Periplasmic and spheroplast fractions were prepared and analyzed by SDS-PAGE and immunoblotting as described in Materials and Methods. To the right of each panel, the primary antibody used is indicated. Lane 1 in all panels contains molecular mass standards. periplasmic fraction; s, spheroplasts (cytosol and membranes). (A) Lanes 2 and 3, $S^{21}68_{TMD1}\Phi Lyz_{\Delta SAR}$. (B) Lanes 2 and 3, PhoA. (C) Lanes 2 and 3, R^{λ}. PhoA and R^{λ} were used as internal controls for periplasmic and spheroplast fractions, respectively.

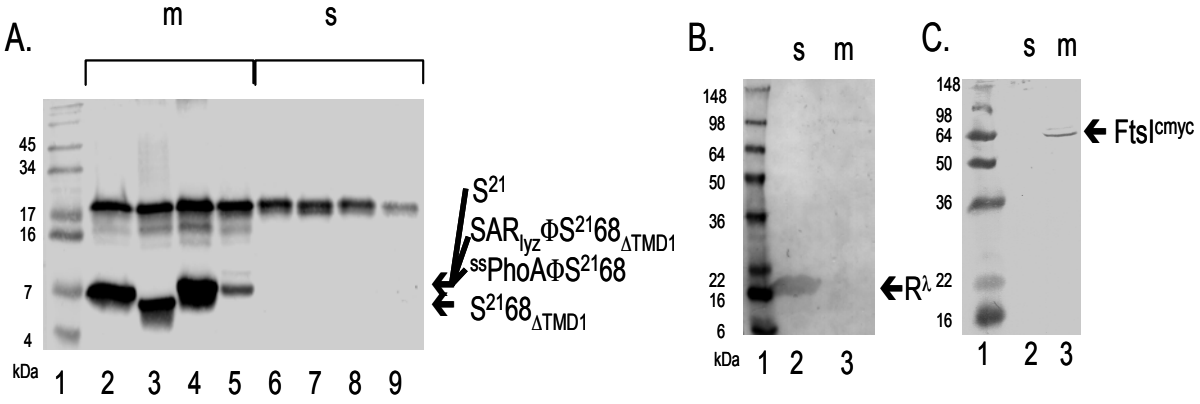

Figure 11. $S^{21}68$ and its derivatives are localized to the membrane. Total membrane and soluble fractions were prepared and analyzed by SDS-PAGE and immunoblotting as described in Materials and Methods. To the right of panel, the primary antibody used is indicated. Lane 1 in all panels contains molecular mass standards. m, membrane fraction; s, soluble fraction. (A) Lanes 2 and 6, $S^{21}68$; lanes 3 and 7, $S^{21}68_{\Delta TMD1}$; lanes 4 and 8, $SAR_{lyz}\Phi S^{21}68_{\Delta TMD1}$; lanes 5 and 9, $^{ss}PhoA\Phi S^{21}68$. (B) Lanes 2 and 3, R^{λ}. (C) Lanes 2 and 3, $FtsI^{cmyc}$. R^{λ} and $FtsI^{cmyc}$ were used as internal controls for soluble and membrane fractions, respectively.

II.2.6. SDS/PAGE and Western blotting

SDS/PAGE and Western blotting were performed as described (Gründling *et al.*, 2000a), except that Tris-Tricine SDS-PAGE (Schägger and von Jagow, 1987) was used for detection of proteinase K degradation products. Antibody against the peptide KIREDRRKAARGE, which corresponds to the S^{21} C-terminus, was raised in rabbits (Barenboim *et al.*, 1999). Proteins tagged with the *cmyc* epitope were detected by using a mouse monoclonal antibody from Babco (Richmond, CA). Antibody against the purified His_6-tagged Lyz was prepared in chickens by Aves Labs, (Tigard, OR). Horseradish peroxidase-conjugated secondary antibodies against chicken IgY, mouse IgG, and rabbit IgG were from Aves Labs, Pierce, and Pierce, respectively. Generally, primary antibodies were used at a 1:1000 dilution, whereas secondary antibodies were used at a 1:3000 dilution. Blots were developed by using the chromogenic substrate 4-chloro-1-naphthol (Sigma). Equivalent sample loadings were used whenever multiple fractions obtained from the same culture were analyzed. For Figure 14D, the Vectastain ABC-AmP kit from Vector laboratories (Burlingame, CA) was used for detection of proteins on the blot.

To show the presence of disulfide-linked dimers of the cysteine-containing derivatives of S^{21}, culture aliquots were adjusted to 10% TCA and placed on ice for 30 minutes. The precipitate was collected by centrifugation and washed with acetone to remove the TCA. Pellets were air-dried and resuspended in SDS-PAGE loading buffer with, or without reducing agent as indicated.

II.2.7. Purification and N-terminal sequencing of $S^{21}68$

$S^{21}68^{his}$ was purified from an induced culture of *E. coli* BL21(DE3) cells carrying the plasmid $pETS^{21}68^{his}$ (Table 1) by immobilized metal ion affinity chromatography, as previously described (Smith *et al.*, 1998a; Deaton *et al.*, 2004). Samples containing approximately 100 μg of $S^{21}68^{his}$ were subjected to SDS-PAGE and the separated proteins were electroblotted onto polyvinylidene fluoride paper (PVDF, Millipore, Bedford, MA). The region of the blot corresponding to the $S^{21}68^{his}$ protein was excised and the bound protein was subjected to automated N-terminal sequencing.

II.3. Results

II.3.1. Topology of nascent S^{21}

Because of the distribution of positively charged residues along the $S^{21}68$/$S^{21}71$ polypeptide chains, the N- and C- termini are both expected to reside in the cytoplasm of the cell (Sonnhammer *et al.*, 1998). Support for this model was obtained by analyzing the N-terminus of purified $S^{21}68$. *$S^{21}68$*, an allele of S^{21} modified to produce only the $S^{21}68$ protein (Figure 9C), was further altered by inserting a DNA sequence encoding an oligohistidine tag between codons 66 and 67 (Figure 9A). When the resultant allele, *$S^{21}68^{his}$*, was expressed and the protein product purified by immobilized-metal ion chromatography, N-terminal sequencing gave the sequence MDKIS with a 94% yield at the first cycle. This indicates that the N-terminus of $S^{21}68$ resides initially in the cytoplasm where it serves as a substrate for the cytoplasmic deformylase. In contrast, the N-terminus of TMDs that rapidly exit the cytoplasm and transit the bilayer, like TMD1

of Lep (von Heijne, 1989) or S105 (R. White, J. F. Deaton, A. Gründling, T. A. T. Tran, and R. Young, in preparation) retain their fMet residues.

II.3.2. TMD1 has the properties of a SAR domain

Since TMD1 of nascent S^{21} is initially membrane-embedded, the topological relationship that exists between the λ holin and antiholin is not possible for their phage 21 analogs. This, however, does not preclude the possibility that the primary distinction between $S^{21}68$ and $S^{21}71$ is topological. TMD1 of the $S^{21}68$/$S^{21}71$ proteins has a composition rich in Gly, Ala, Ser, and Thr, similar to the SAR domains of the P1 and 21 endolysins (Figure 9A), raising the possibility that TMD1 behaves as a SAR domain and leaves the bilayer as part of its function (Figure 9B). To determine whether the TMD1 of S^{21} could function as a SAR domain outside of the holin context, we substituted it for the SAR domain of Lyz, the endolysin of bacteriophage P1 (Figure 9A). Subcellular fractionation of cells expressing $S^{21}68_{TMD1}\Phi Lyz_{\Delta SAR}$ demonstrated that, like the wild type Lyz protein, the chimeric protein existed as both membrane-bound and soluble forms with identical mass (Figure 12A). Moreover, some of the soluble form was periplasmic (Figure 10) consistent with the initial integration of the chimera with an N-in, C-out topology followed by its subsequent release from the membrane into the periplasm.

Table 1. Plasmids used in this work

Plasmid	Features	Source or reference
pS105	pBR322 origin, pR′ promoter and *S105RRzRz1* from λ	(Gründling *et al.*, 2001)
pQ	pSC101 origin with modification, $P_{lac/ara-1}$ promoter, *Q* from λ	(Gründling *et al.*, 2001)
pBP71	pBR322 origin, pR′ promoter and *QS71RRzRz1* from phage 21, expressing only $S^{21}71$ from S^{21} gene	(Barenboim *et al.*, 1999)
pBP68	pBR322 origin, pR′ promoter and *QS68RRzRz1* from phage 21, expressing only $S^{21}68$ from S^{21} gene	(Barenboim *et al.*, 1999)
pTP1	*S105RRzRz1* of pS105 replaced with *S71RRzRz1* of pBP71	this study
pTP2	*S105RRzRz1* of pS105 replaced with *S68RRzRz1* of pBP68	this study
pTP3	pTP2 with $S^{21}68_{amber}$	this study
pTP4	pTP2 with $R^{21}_{double\ amber}$	this study
pTP5	pTP2 with codons of $S^{21}68_{TMD1}$ replaced with ones of SAR domain of P1 Lyz	this study
pTP6	pTP2 with codons of signal sequence of alkaline phosphatase inserted between codons 1 and 2 of $S^{21}68$	this study
pTP7	pTP2 encoding RYIRS fusion to N-terminus of $S^{21}68$	this study
pTP8	pTP2 encoding $S^{21}68_{TMD1}$ fusion to SAR domain-less P1 Lyz	this study
pTP9	pTP5 encoding RYIRS fusion to N-terminus of $S^{21}68_{TMD1}$ΦLyz$_{\Delta SAR}$	this study
pJFLyz	pJF118 with P1 *lyz*	(Xu *et al.*, 2004)
pJFFtsI	pJF118 encoding *c-myc* tag fused to FtsI	(Xu *et al.*, 2004)
pJFPhoA	pJF118 encoding PhoA	(Xu *et al.*, 2004)
pR^{λ}	pJF118 encoding R^{λ}	(Xu *et al.*, 2004)
$pETS^{21}68^{his}$	pET11a carrying $S^{21}68$ gene of pBP68 at NdeI-HindIII restriction enzyme site with introduction of codons of GGH_6GG between codons 66 and 67.	Deaton J. and Barenboim M., unpublished data

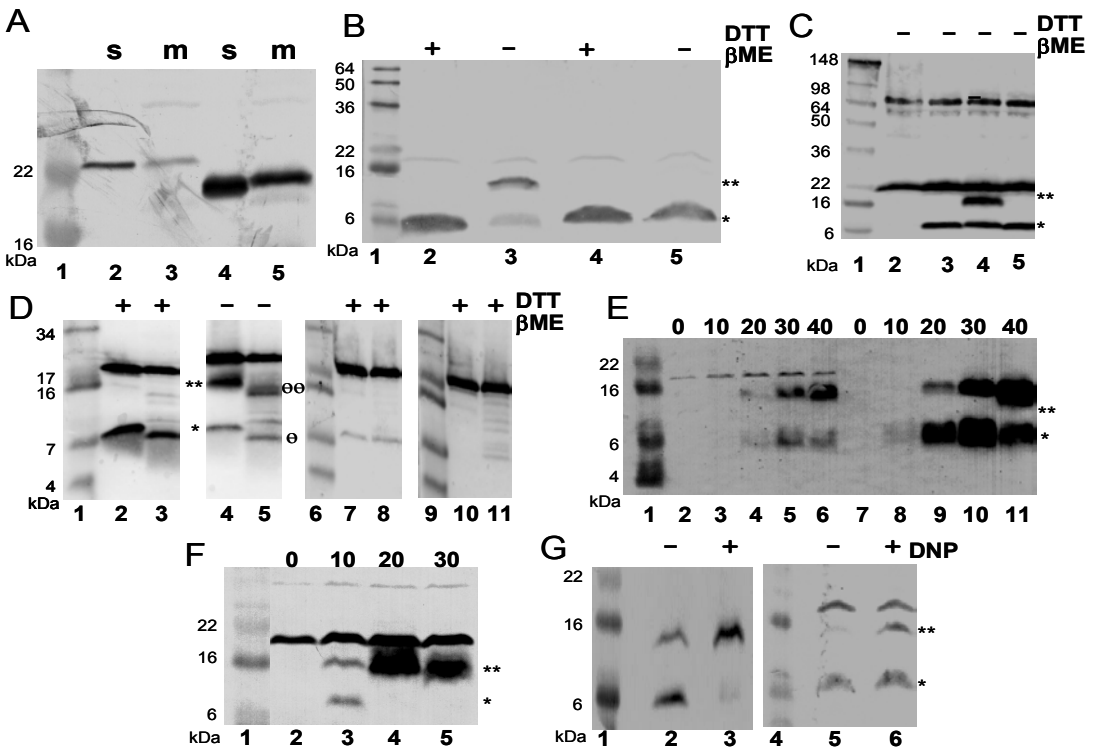

Figure 12. TMD1 exits the membrane. Aliquots from cultures expressing the indicated genes were collected by TCA precipitation and analyzed by SDS-PAGE under reducing or non-reducing conditions, as indicated. Except for panel A, where anti-Lyz antisera were used, separated proteins were detected by Western blotting using antisera raised against the C-terminal peptide of S^{21}. Lane 1 in all panels, lane 6 and 9 in panel D and lane 4 in panel G contain molecular mass standards. In panels B-G, a star and a double star indicate the positions of the monomer and dimer forms of $S^{21}68_{S16C}$, respectively. (A) TMD1 of $S^{21}68$ can substitute for the SAR domain of P1 Lyz. Lanes 2 and 3, $S^{21}68_{TMD1}\Phi Lyz_{\Delta SAR}$; lanes 4 and 5, *lyz*; m, membrane fraction; s, soluble fraction. FtsI and R^{λ} were used as controls for the membrane and soluble fractions, respectively (Figure 11). (B) Dimerization of $S^{21}68_{S16C}$ via its TMD1. Lanes 2 and 3, $S^{21}68_{S16C}$; lanes 4 and 5, $RYIRS\Phi S^{21}68_{S16C}$. Samples taken at 40 min after induction were prepared with or without the reducing agents DTT and β-mercaptoethanol, as indicated. (C) Disulfide formation reflects specific TMD1-TMD1 interactions. Lane 2, vector control; lane 3, $S^{21}68$; lane 4, $S^{21}68_{S16C}$; lane 5, $S^{21}68_{G14C}$. (D) Protease sensitivity of $S^{21}68_{S16C}$ dimers. In this panel, a large format Tris-Tricine gel system was used to allow resolution of the dimer- and monomer-related degradation products. Spheroplasts were prepared, induced for the expression of the indicated $S^{21}68$ allele, and subsequently digested with proteinase K as described in Materials and Methods. Lanes 2-5, spheroplasts expressing $S^{21}68_{S16C}$ and treated with protease for 0 (lanes 2 and 4) or 5 minutes (lanes 3 and 5); in lanes 2 and 3, the sample loading buffer contained reducing agents. Lanes 7-8, spheroplasts expressing $RYIRS\Phi S^{21}68_{S16C}$ and treated with protease for 0 (lane 7) or 5 minutes (lane 8). Lanes 10-11, induced spheroplasts carrying the plasmid vector treated with protease for 0 (lane 10 or 5 minutes (lane 11). Symbols θθ and θ to the right of lane 5 indicate the position of the major degradation product of the dimer and monomer forms, respectively. A solid circle to the right of lane 8 indicates the position of the RYIRSΦ$S^{21}68_{S16C}$ monomer form. (E) Dimerization of S^{21} proteins increases as a function of time after induction. Lanes 2-6, $S^{21}68_{S16C}$; lanes 7-11, $S^{21}71_{S16C}$. Samples were taken at the times (minutes) indicated above the lanes and subjected to SDS-PAGE without reduction. (F) Direct export of TMD1 accelerates dimerization of the S^{21} holin. Lanes 2-5, $^{ss}phoA\Phi S^{21}68_{S16C}$. Samples were taken at indicated times (minutes) and subjected to SDS-PAGE without reduction. (G) Collapse of the membrane potential accelerates dimerization of S^{21} proteins. 20 minutes after induction, DNP was added to one of duplicate cultures expressing either $S^{21}68_{S16C}$ or $S^{21}71_{S16C}$. 5 minutes later, samples were taken from all four cultures and subjected to SDS-PAGE without reduction. Lanes 2 and 3, $S^{21}68_{S16C}$; lanes 5 and 6, $S^{21}71_{S16C}$.

II.3.3. TMD1 is not required for S^{21} holin function

Since TMD1 is capable of exiting the bilayer, it seemed possible that the hole-forming activity of S^{21} might reside exclusively in TMD2. To test this possibility, we deleted all of the codons for TMD1 from *$S^{21}68$*. The resulting construct, *$S^{21}68_{\Delta TMD1}$* (Figure 9A), encodes a bitopic membrane protein of only 44 residues. $S^{21}68_{\Delta TMD1}$ accumulates exclusively in the membrane (Figure 11) and was similar to $S^{21}68$ in inducible lethality, triggering at a defined time and causing activation of R^{21}, the phage 21 endolysin (Figure 13A and B). Moreover, as is characteristic of all holins, both $S^{21}68$ and $S^{21}68_{\Delta TMD1}$ could be triggered prematurely by the addition of the energy poison, dinitrophenol (DNP) (Figure 13A and B). Since the expression of the SAR endolysin gene, *R^{21}*, even in the absence of holin function can result in cell lysis (Figure 13A), the lethality of the $S^{21}68_{\Delta TMD1}$ protein was also determined using a plasmid encoding the inactive E35Q allele of *R^{21}*. In this experiment, the triggering of the holin to form a lethal membrane lesion is indicated by the cessation of culture growth. As can be seen in Figure 13C, *$S^{21}68_{\Delta TMD1}$* retains the inducible lethality of the full length holin, although the time of triggering is delayed compared to the wild type.

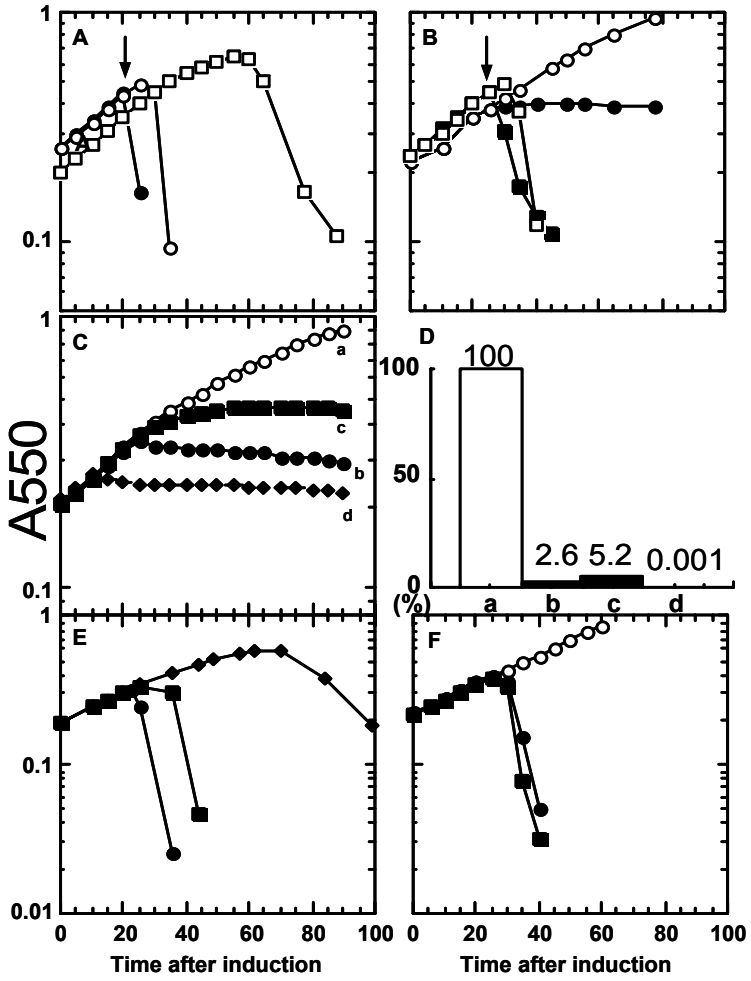

Figure 13. The TMDs of $S^{21}68$ have opposing functions. In each experiment, cultures of MG1655 *lacI*^{q1} *tonA::*Tn*10* bearing a plasmid carrying the indicated S^{21} and R^{21} alleles under the control of the λ late promoter, pR', and a compatible transactivating plasmid, pQ, carrying the λ late activator gene *Q* under the control of a hybrid *lac-ara* promoter (Table 1). The cultures were induced at time 0 and turbidity was followed as a function of time. Constructs used in panels A, B, E and F contained the wild type R^{21} gene, while those used in panel C carried, instead, $R^{21}{}_{E35Q}$, encoding an enzymatically inactive form of R^{21}. (A) Expression of $S^{21}68$ in combination with R^{21} results in abrupt host lysis. (●,○), $S^{21}68\ R^{21}$; □, $S^{21}68am\ R^{21}$. DNP was added (arrow) to one culture (●) at 20 minutes after induction. (B) Expression of $S^{21}68_{\Delta TMD1}$ in combination with R^{21} results in abrupt host lysis. (●,○), vector control; (■,□), $S^{21}68_{\Delta TMD1}\ R^{21}$; DNP was added (arrows) to two of the cultures (■,●) at 25 minutes after induction. (C, D) Induction of different $S^{21}68$ alleles in the absence of endolysin causes lethality. Panel C shows growth curves following induction: (○, curve a), vector control; (●, curve b), $S^{21}68$; (■, curve c)), $S^{21}68_{\Delta TMD1}$; (◆, curve d), $^{ss}phoA\Phi S^{21}68$. Panel D shows cell survival at 60 min after induction, assessed as colony forming units (CFU) and expressed as a percentage of the control. (E) TMD1 of $S^{21}68$ antagonizes the holin activity of its TMD2. (●), $S^{21}68\ R^{21}$; (■), $S^{21}68_{S16C}R^{21}$; (◆), $RYIRS\Phi S^{21}68_{S16C}\ R^{21}$. (F) The SAR domain of P1 Lyz cannot inhibit hole-formation by TMD2 of $S^{21}68$. (○), $SAR_{lyz}\Phi S^{21}68_{\Delta TMD1}$, uninduced; (●), $SAR_{lyz}\Phi S^{21}68_{\Delta TMD1}$, induced; (■) , $RYIRS\text{-}SAR_{lyz}\Phi S^{21}68_{\Delta TMD1}$, induced.

II.3.4. Does TMD1 exit the bilayer?

To provide biochemical evidence that TMD1 of nascent, membrane-inserted $S^{21}68$ leaves the bilayer, we altered the S^{21} gene so that codon 16 encodes Cys rather than Ser (Figure 9A). Our rationale was that disulfide-linked dimers might form if oligomerization of the holin in the membrane brought the TMD1 segments from many $S^{21}68$ molecules into close proximity in the oxidizing environment of the periplasm. Induction of the $S^{21}68_{S16C}$ missense allele in the presence of R^{21} resulted in abrupt lysis of the host, indicating that the S16C protein is fully functional as a holin (Figure 13E). The fact that the $S^{21}68_{S16C}$ allele triggers 5-10 minutes later than the wild type is not unexpected, given the wide range of lysis times seen with a collection of single missense mutants in the holin of bacteriophage λ (Raab *et al.*, 1988). When membranes of cells expressing the $S^{21}68_{S16C}$ allele were examined by SDS-PAGE under nonreducing conditions, a dimeric species was identified by Western blot analysis (Figure 12B). Moving the Cys residue to the opposite face of the putative TMD1 helix eliminated the dimer (Figure 12C), suggesting that its formation is due to specific TMD1-TMD1 interhelical interactions. We next inserted an oligonucleotide sequence encoding the epitope RYIRS after the start codon of $S^{21}68_{S16C}$ (Figure 9A). The presence of the additional positive charges provided by this epitope at the N-terminus of $S^{21}68$ should prevent its TMD1 from leaving the membrane. The RYIRS-tagged protein ran as a monomer under both reducing and nonreducing conditions (Figure 12B), consistent with the retention of its TMD1 in the membrane.

Additional support for our contention that TMD1 of S^{21} moves from the membrane to the periplasm was obtained by examining the protease sensitivities of the $S^{21}68_{S16C}$ and RYIRS-tagged $S^{21}68_{S16C}$ in spheroplasts. Upon exposure to proteinase K, the majority of the $S^{21}68_{S16C}$ dimer was converted to a form that migrated between the dimer and monomer positions when analyzed by non-reducing SDS-PAGE (Figure 12D, compare lanes 4 and 5). The mobility of this cleavage product increased upon reduction, indicating the presence of a disulfide bond (Figure 12D, compare lanes 3 and 5). Moreover, the small amount of monomer present was also converted into a form that had a slightly faster mobility. Since the Western blot was developed with antibodies raised to a peptide corresponding to the C-terminal 13 residues of S^{21}, the bands visualized must have resulted from cleavage between the N-terminus and Cys16 and, thus, within TMD1. The RYIRS-tagged $S^{21}68_{S16C}$ protein was found to be protease resistant (Figure 12D, compare lanes 7 and 8). The different protease sensitivity of TMD1 in $S^{21}68$ and the RYIRS-tagged protein supports our interpretation that the former is exposed to the aqueous environment while the latter remains embedded in the membrane.

II.3.5. Membrane-inserted TMD1 specifically inhibits hole formation by TMD2

Surprisingly, cells induced to synthesize the RYIRS-tagged $S^{21}68_{S16C}$ grew well past the time of triggering for $S^{21}68_{S16C}$ (Figure 13E). This suggests that the presence of TMD1 of $S^{21}68$ in the membrane blocks lesion formation by TMD2. To show that this inhibitory effect was specific, we replaced TMD1 of $S^{21}68$ with the SAR domain of Lyz (Figure 9A). The chimeric protein, $SAR_{lyz}\Phi S^{21}68_{\Delta TMD1}$, retained its holin function

although triggering was delayed about 5 min when compared to $S^{21}68$ (Figure 13F). Unlike the case of $S^{21}68$, attaching the RYIRS-tag to the N-terminus of the $SAR_{lyz}\Phi S^{21}68_{\Delta TMD1}$ protein did not alter the triggering time of the chimera (Figure 13F). Thus, the inhibition of hole formation is specific for the SAR domain of S^{21} and is not observed with a heterologous SAR domain. Further support for the idea that TMD1 serves physiologically as an inhibitor of hole formation was obtained by fusing the cleavable signal sequence from the periplasmic enzyme alkaline phosphatase (PhoA) to the N-terminus of $S^{21}68$ (Figure 9A). Expression of this construct, *$^{ss}phoA\Phi S^{21}68$*, was lethal much earlier than with wild type *$S^{21}68$* (Figure 13C and D). SDS-PAGE and Western blotting showed that the chimeric protein had been processed by signal peptidase and migrated identically to $S^{21}68$ (Figure 11). We suspect that the early lethality of the $^{ss}PhoA\Phi S^{21}68$ protein is due to the fact that the SAR domain that constitutes TMD1 of $S^{21}68$ was exported directly to the periplasm and never resided in the membrane (see below).

II.3.6. Exit of TMD1 from the membrane coincides with holin triggering

Finally, to demonstrate that TMD1 of the *S^{21}* gene products spends a discrete period of time in the inner membrane before its release to the periplasm, we followed the change in the monomer/dimer ratio for the S16C alleles of *$S^{21}68$* and also for *$S^{21}71$*, an allele that produces only the antiholin (Figure 9C; see Materials and Methods), as a function of time. As can be seen in Figure 12E, the relative amount of the dimeric species increased with time for both proteins. With $^{ss}PhoA\Phi S^{21}68_{S16C}$, where a secretory

signal sequence directly effects export of TMD1, the kinetics of disulfide bond formation is accelerated (compare Figure 12E to 12F) as is the kinetics of triggering (Figure 13C). Moreover, artificially triggering either the holin or the antiholin by the addition of the uncoupler, DNP, resulted in a rapid and dramatic increase in the amount of dimerized S^{21} (Figure 12G).

II.4. Discussion

II.4.1. Topological differences between the S^{21} holin and antiholin

The *S*^{21} gene encodes two proteins with two predicted TMDs; S^{21}68, a holin, and S^{21}71, an antiholin. TMD1 of S^{21} is enriched for small, nonpolar (Ala, Gly) and polar, uncharged (Thr, Ser) residues, a feature unusual for canonical TMDs but common to the established SAR domains of the bacteriophage endolysins, Lyz and R^{21} (Xu *et al.*, 2004). The N-terminal SAR domains of the latter proteins facilitate their secretion to the periplasm where they remain tethered to the cytoplasmic membrane via their SAR helices. Subsequently, their SAR domains exit the membrane, thereby releasing active endolysin to the periplasm (Xu *et al.*, 2004). If the S^{21} TMD1 behaved as a SAR domain, then the S^{21} holin would have one fewer TMD than its antiholin (Figure 9B).

Several lines of evidence support this model. First, and most surprising, deletion of TMD1 from S^{21}68 did not abolish its holin function but only delayed its triggering time by about 5 min (compare Figure 13A to 13B). This makes $S^{21}68_{\Delta TMD1}$, at 44 residues, the smallest polypeptide known to exhibit the essential properties of a holin. Secondly, its deformylated state places the N-terminus of nascent S^{21} in the cytoplasm,

both the propensity of $S^{21}68_{S16C}$ to form disulfide-linked dimers (Figure 12B) and the protease sensitivity of the dimers in spheroplasts (Figure 12D) places TMD1 in the periplasm. Moreover, while most of either $S^{21}68_{S16C}$ or $S^{21}71_{S16C}$ protein exists as a monomer shortly after induction, the proportion that exists as a dimer increases with time (Figure 12E). Dimer formation occurs most rapidly with $S^{21}68$, perhaps due to the extra positively charged residue at the N-terminus of $S^{21}71$ which serves to impede the release of its TMD1 to the periplasm. A critical prediction of our model is that treatments known to artificially trigger S^{21} should result in a rapid increase in the amount of dimer. Indeed, the addition of DNP to cultures induced for either protein increased the amount of dimer. Significantly, the conversion of $S^{21}68$ monomer to dimer was immediate and nearly complete (compare lanes 2 and 3 of Figure 12G). This strongly argues that the rate at which the S^{21} dimers appear reflects the rate at which the membrane-embedded TMD1 enters the periplasm. These experiments indicate that TMD1 of both $S^{21}68$ and $S^{21}71$ is initially inserted into the cytoplasmic membrane and is subsequently released to the periplasm.

II.4.2. Role of TMD1 in holin triggering

Since TMD1 is not essential for the holin function of $S^{21}68$, what, then, is its function? The behavior of the RYIRS-tagged $S^{21}68_{S16C}$ protein suggests an answer to this question. SDS-PAGE and Western blotting showed that, while the tagged protein was present at normal levels, the disulfide-linked dimer was notably missing (Figure 12B). We interpret this to mean that the additional positive charges provided by the

RYIRS tag prevent the movement of TMD1 from the membrane to the periplasm. Significantly, cells producing this protein grew well beyond the point at which lysis would have occurred due to the induction of $S^{21}68_{S16C}$ (Figure 13E). Thus, the continued presence of TMD1 in the membrane was antagonistic towards the lesion-forming activity of TMD2.

II.4.3. Model for the function of S^{21}

Both of the S^{21} TMDs have potential GxxxG-like motifs (Figure 9A and 12A) that might serve as the basis for homotypic and/or heterotypic helix interactions (Senes *et al.*, 2004). GxxxG-like motifs have been implicated in such interactions between transmembrane helices by facilitating the intimate approach of the polypeptide backbones and the formation of H-bonds between αH atoms and backbone carbonyls (Senes *et al.*, 2000; Senes *et al.*, 2001). For TMD1, these motifs provide a glycine-rich surface which may be important for interhelix packing, particularly in the periplasm. For the TMD2 helix, the contact surface defined by its two overlapping GxxxG-like motifs is coincident with its single hydrophilic surface (Figure 14A) which could line the "hole" formed by S^{21} after triggering.

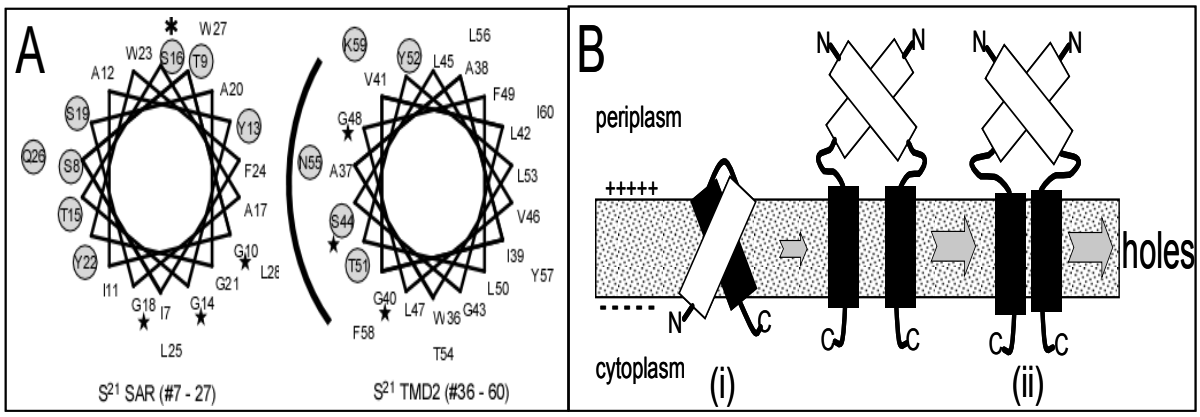

Figure 14. Potential homotypic and heterotypic TMD interactions in the function of S^{21}. (A) Helical projections of TMDs of S^{21}. Stars indicate GxxxGxxxG-like motifs of each TMD (G10, G14 and G18 in TMD1; G40, S44, G48 in TMD2). Hydrophilic or neutral residues in each TMD are circled and shaded. Left: the SAR domain (TMD1) of S^{21} (residues 7-27), with the position of the S16C mutation highlighted by an asterisk. Right: TMD2, the hole-forming domain of S^{21} (residues 36-60), with a potential hydrophilic surface that may line the lethal membrane lesion indicated by the arc. (B) Pathway to hole formation involves inhibited (i) and active (ii) topological isomers of S^{21}. See text for details.

Our model for hole formation by S^{21} is depicted in Figure 14B. Initially, S^{21} is inserted into the cytoplasmic membrane as a helical hairpin with predominant TMD1-TMD2 interactions. These interactions either mask the hydrophilic surface of TMD2 or prevent the self-association of TMD2 and serve to block hole formation. Upon triggering, TMD1 exits the membrane for the periplasm, allowing oligomerization of S^{21} via homotypic TMD2-TMD2 interactions within the bilayer, a process that might be facilitated by homotypic TMD1-TMD1 interactions in the periplasm. By this reasoning, the delayed triggering of $S^{21}68_{\Delta TMD1}$ (Figure 13B) and $SAR_{lyz}\Phi S^{21}68_{\Delta TMD1}$ (Figure 13F) would be due to the absence of the periplasmic TMD1 interactions. The antiholin

activity of $S^{21}71$ is due to the extra positive charge at its N-terminus (Figure 9) that delays the exit of its TMD1 from the membrane compared to $S^{21}68$. The presence of significant levels of $S^{21}71$ in its helical hairpin configuration with interacting TMDs would "poison" the oligomerization of $S^{21}68$ into functional holes.

There are many issues of interest that arise from this perspective. First, it is not clear what allows a SAR domain to escape from the membrane in a potential-dependent manner. Also, neither for S^{λ} nor for S^{21} is it understood what constitutes the timing mechanism that allows holins to impose a specific temporal program on the infective cycle. Our model for S^{21} predicts that the escape of TMD1 is necessary for holin triggering, but it is clearly not sufficient. Even the $S^{21}68_{\Delta TMD1}$ deletion protein, lacking the inhibitory TMD1, still has a defined triggering time. And, finally, it is unclear how the timing mechanism of either holin is subverted by de-energization of the membrane.

CHAPTER III

THE PINHOLIN GENE OF LAMBDOID PHAGE 21: CONTROL OF LYSIS BY MEMBRANE DEPOLARIZATION

III.1. Introduction

For most phages, the termination of each infection cycle is the strictly programmed and regulated lysis of the host brought about by two phage-encoded proteins. One of these, the endolysin, is capable of degrading the cell wall while the second, the holin, is a small membrane protein which controls endolysin function. During the assembly of progeny virions, holin molecules accumulate in the cytoplasmic membrane without damaging the host. Then, at a time dictated by their primary structure, holins trigger to disrupt the cytoplasmic membrane. For many phages, like λ and T4, this event allows the release to the periplasm of an endolysin which has accumulated fully folded and enzymatically active in the cytosol. By contrast, phages P1 and 21 encode endolysins that are exported by the host *sec* system and accumulate in the periplasm as enzymatically inactive proteins tethered to the membrane by an N-terminal SAR (signal-anchor-release) domain (Xu *et al.*, 2004). The SAR endolysins become enzymatically active when their SAR domains exit the membrane to generate the mature, soluble form in the periplasm. This process occurs spontaneously at a slow rate but is greatly accelerated when the cytoplasmic membrane is de-energized. Thus, for phage encoding SAR endolysins, holins need only to depolarize the membrane in order to fulfill their role in controlling the timing of lysis. Forming large membrane lesions, as has been shown with S^{λ}, would not be necessary. This raises the possibility

that holins serving SAR endolysins may not function with canonical, soluble endolysins to effect saltatory host lysis.

III.2. Materials and methods

III.2.1. Bacterial strains, phages, and culture conditions

All bacterial cultures were grown in standard LB medium, supplemented with various antibiotics when appropriate: ampicillin, 100 μg/ml; chloramphenicol, 25 μg/ml; kanamycin, 40μg/ml; and tetracycline, 10 μg/ml. When indicated, isopropyl β-D-thiogalactoside (IPTG), arabinose or $CHCl_3$ were added at final concentration of 1mM, 0.2% or 1%, respectively. When indicated, thermal induction for the phages was used as previously described (Barenboim *et al.*, 1999; Raab *et al.*, 1988; Ramanculov and Young, 2001a; Tran *et al.*, 2005; Xu *et al.*, 2004).

Standard conditions for the growth of cultures and the monitoring of lysis kinetics have been described (Chang *et al.*, 1995; Smith *et al.*, 1998b). With an exception of figure 16A, all experiments were done with a *tonA::*Tn*10* derivative of MDS12, the sequenced *E. coli* K-12 strain, and its lysogens. In figure 16A, experiment was performed with various lysogens of MC4100. To make *λ-21* hybrid phages, an established recombination strategy was used as previously described (Barenboim *et al.*, 1999; Ramanculov and Young, 2001a; Tran *et al.*, 2005). All bacterial strains and phages used in this study were explained in Table 2.

Table 2. Bacterial strains, bacteriophages, and plasmids used in this study

Strain, phage, or plasmid	Genotype and relevant features	Source or reference
Strains		
MC4100	*E. coli K-12 F⁻ araD139 Δ(argF-lac)U169 rpsL150 relA1 flbB5301 deoC1 ptsF25 rbsR*	(Kiino and Silhavy, 1984)
MC4100 λ*kan*Δ(*SR*)	Lysogen carrying λ*kan*Δ(*SR*) prophage	(Raab *et al.*, 1988)
MG1655	F⁻ *ilvG rfb50 rph1*	E. coli Genetic Stock Center
MDS12	MG1655 with 12 deletions, totaling 376,180 nt, including cryptic prophages	(Kolisnychenko *et al.*, 2002)
MDS12 tonA::Tn10	*tonA::Tn10* version of MDS12	This study
Phages		
λ111	λ *cI857* S_{am}*7RRzRz1*	(Goldberg and Howe, 1969)
λ81	λ *cI857* $SR_{double\ amber}$ *RzRz1*	Laboratory stock
λ*Cam*Δ(*SR*)	*stf::cat::tfa cI857* Δ(*SR*)	(Smith and Young, 1998a)
λ*Cam*(*S68RRzRz1*)^{21}	λ-21 hybrid phage carrying *S68RRzRz1* of phage 21 under $\lambda P_R'$	This study
λ*Cam*(*S68R-RzRz1*)^{21}	λ-21 hybrid phage carrying $S68R_{double\ amber}$*RzRz1* of phage 21 under $\lambda P_R'$	This study
λ*Cam*(*S68-RRzRz1*)^{21}	λ-21 hybrid phage carrying $S68_{ambe}R_{,}$*RzRz1* of phage 21 under $\lambda P_R'$	This study
Plasmids		
pBP68	pBR322 origin, P_R' promoter and *QS68RRzRz1* from phage 21, expressing only $S^{21}68$ from S^{21} gene	(Barenboim *et al.*, 1999)
pKB110	pBR322 origin, P_R' promoter and *SRRzRz1* from λ	(Smith and Young, 1998a)
pS105	pBR322 origin, P_R' promoter and *S105RRzRz1* from λ	(Smith and Young, 1998a)
pRE	pBR322 origin, P_R' promoter	Chapter II
pTP2	*S105RRzRz1* of pS105 replaced with *S68RRzRz1* of pBP68	Chapter II
pTP3	pTP2 with codon for valine at position 43 of S68 changed to amber codon	This study
pTP4	pTP2 with $68R_{double\ amber}$ RzRz1	This study
$P_R'(S105R_{ochre,\ amber}RzRz1)^{\lambda}$	$S105R_{ochre,\ amber}$RzRz1	Laboratory stock
pJFLyz	pJF118 plasmid encoding P1*lyz*	(Xu *et al.*, 2004)
pR^{λ}	pJF118 plasmid encoding R^{λ}	(Xu *et al.*, 2004)
pJFT4E	pJF118 plasmid encoding T4E	(Xu, M., unpublished data)
pTGS	TorA leader peptide fused to SsrA-tagged GFP in pBAD33	(DeLisa *et al.*, 2002)

III.2.2. Standard DNA manipulation, PCR, and DNA sequencing

Procedures for the isolation of plasmid DNA, DNA amplification by PCR, PCR product purification, DNA transformation, and DNA sequencing have been described (Smith *et al.*, 1998a; Smith and Young, 1998b; Gründling *et al.*, 2000a). Oligonucleotides were obtained from Integrated DNA Technologies, Coralville, IA, and were used without further purification. Ligation reactions were performed by using the Rapid DNA ligation kit from Roche Molecular Biochemicals according to the manufacturer's instructions. All other enzymes were purchased from Promega, with the exception of *Pfu* polymerase, which was from Stratagene. Automated fluorescent sequencing was performed at the Laboratory for Plant Genomic Technologies in the Crop Biotechnology Center at Texas A&M University.

III.2.3. Plasmids and induction

For most experiments, the bacterial strains and its lysogen carried a medium copy plasmid with a pBR322 origin and the lysis gene cassette, *SRRzRz1*, under the control of the λ late promoter, pR' (Gründling *et al.*, 2000c). The lysis gene cassettes were either from λ or phage 21, as indicated. Expression of the lysis genes was accomplished by inducing λ prophage by a thermal induction. Briefly, the culture was grown at 30^{o}C to A550 of 0.2, thermally induced by transfer to 42^{o}C for 15 min, and further incubated at 37^{o}C. When induced, the λ antiterminator Q is expressed from either λ or λ-21 hybrid prophages, which transactivates $\lambda P_R'$ promoter on the plasmid. Expression of the lysis

genes follows transactivation of P_R' by Q. The various *S*^{21}*68* alleles used in this study were expressed in constructs based on the plasmid pS105, which is a pBR322 derivative carrying the λ late promoter, $p_{R'}$, and the entire λ lysis cassette, *SRRzRz1*, on an EcoRI-ClaI fragment. The promoter is activated when the pR' activator Q is supplied from the thermal induction of either λ or λ-21 hybrid phage. The source of phage 21 lysis genes was the plasmid pBP68 (Barenboim *et al.*, 1999), which has an *EcoRI-ClaI* fragment carrying the genes *S*^{21}*68R*^{21}*Rz*^{21}*Rz1*^{21}. *S*^{21}*68* is an allele of the holin gene *S*^{21} in which the Met_1 codon has been changed to Leu (CUG) so that only the S^{21}68 holin gene product is expressed (see chapter II for details). To construct pTP2, the *EcoRI-ClaI* fragment in pS105 was replaced by the corresponding *EcoRI-ClaI* fragment from pBP68. The expression level of the *S*^{21}*68* gene was increased by changing the Shine-Dalgarno sequence from cggaggc to aggaggt (positions -13 to -7 upstream of the *S*^{21} start codon) and deleting the first three codons of the *S*^{21} gene to make the spacing between the modified Shine-Dalgarno sequence and the start codon of the *S*^{21}*68* reading frame similar to that of *S*^{21}*71* gene, using site-directed mutagenesis. The sole *S*^{21} gene product from pTP2 is S^{21}68 (see chapter II for details). Nonsense changes in the *S*^{21} and *R*^{21} genes of pTP2, and others were introduced by conventional site-directed mutagenesis using the QuikChange kit from Stratagene. Construction of pJFLyz and pR$^{\lambda}$ in which *lyz* and *R*$^{\lambda}$ are under *tac* promoter control, respectively, was previously described (Xu *et al.*, 2004). All constructs were verified by DNA sequencing. Where needed, 1mM IPTG or 0.2% arabinose was added to the culture for induction of indicated genes. In experiments where P1 *lyz*, R$^{\lambda}$, or T4E was induced, the only plasmid present was a derivative of

pJF118, a medium copy plasmid carrying the each designated gene under control of the *tac* promoter (Xu *et al.*, 2004). All plasmids used in this study were explained in Table 1.

III.2.4. Plating bacteriophage

Plating of phage *λ-21* hybrid phages were done as described previously (Zhang and Young, 1999). Briefly, 0.1 ml of hybrid phage diluted with λdil (5 mM MgSO4, 0.01 % gelatin, 10 mM Tris-HCl, pH 7.4) was mixed with 0.1 ml of a overnight culture of MDS12 *tonA::Tn10*, grown in TB (supplemented with 0.2% maltose). Then, the mixture was incubated at room temperature for 30 min, mixed with 3 ml of molten T-top agar (supplemented with 10mM $MgSO_4$), and plated on fresh TB plates. Plates were incubated at least 7 h at 37^{o}C before they were scanned by EPSON perfection 4990 Photo scanner. When needed, a plaque was picked, diluted into 0.1 ml of λdil, and sterilized by addition of 1% $CHCl_3$.

III.2.5. Fluorescence Microscopy

An overnight culture of lysogen carrying λ*kan*Δ(*SR*) and indicated plasmids was diluted 1:500 in 25 ml LB and grown until A550 ~ 0.1 at 30^{o}C, when the culture was induced with arabinose. One hundred minutes after the arabinose induction, the cultures were thermally induced for 60 min, collected by centrifugation at 5000 x *g*, washed twice with PBS (137 mM NaCl, 2.7 mM KCl, 10 mM Na_2HPO_4, 2 mM KH_2PO_4, pH 7.4), and resuspended into 500 μl PBS. The cells were examined immediately by Zeiss Axioplan 2 imaging fluorescence microscope.

III.3. Results

III.3.1. R^{21} expression allows holin-independent lysis but not uniform plaque formation

Because of its dual start motif, the S^{21} gene gives rise to two products, $S^{21}71$ and $S^{21}68$. To further characterize the phage 21 holin, $S^{21}68$, and endolysin, R^{21}, we replaced the defective lysis cassette of λΔSR with the $S^{21}68R^{21}Rz^{21}Rz1^{21}$ genes from pTP2 (see chapter II for details) by homologous recombination. The resulting phage, λ$S^{21}68R^{21}$, formed large plaques of uniform size on a standard non-suppresor hosts (Figure 15A). Moreover, in liquid culture, the lysis of induced λ $S^{21}68R^{21}$lysogens displayed a saltatory nature indicative of its holin-mediated timing. The behavior of λ $S^{21}68_{am}R^{21}$ was different with respect to both phenotypes. First, while λ $S^{21}68_{am}R^{21}$ was a plaque former, the plaques were overall smaller and showed considerable size variation

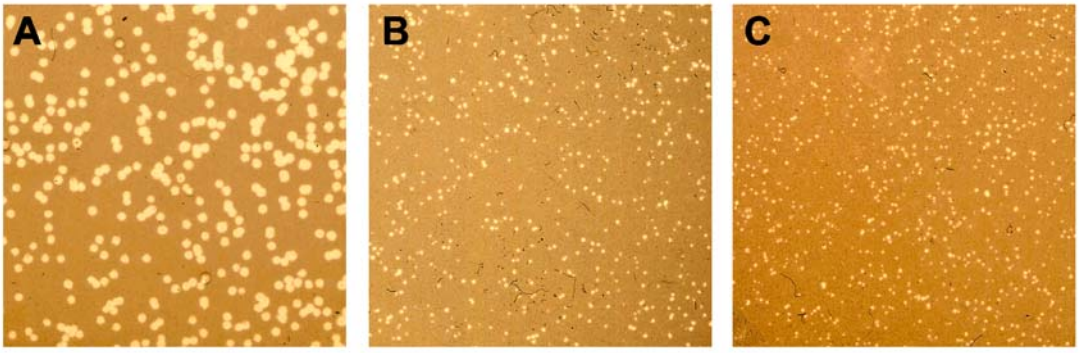

Figure 15. Absence of $S^{21}68$ holin contributes to heterogeneity of plaque morphology. In all panels, MDS12 *tonA::*Tn*10* was used as the indicator lawn for plating, as as described in *Materials and Methods*. Panel A: λ$S^{21}68R^{21}$. Panel B: λ$S^{21}68_{am}R^{21}$. Panel C: replating of a large plaque from the plate shown in Panel B

(Figure 15B). This plaque-size heterogeneity persisted when phage from large and small plaques were replated; Figure C shows the results from replating a large plaque. Second, for induced λ $S^{21}68_{am}R^{21}$ lysogens, lysis in liquid culture is less saltatory, requiring 30-40 minutes for completion as assessed by monitoring the decrease in culture OD_{550} (Figure 16A)

III.3.2. S^{21} and S^{λ} are not functionally equivalent

We next designed experiments to determine if $S^{21}68$ and R^{21} could complement the lysis defect of phages λ*Sam7* and λ*SRam*, respectively. Previously, we had reported that, when expressed from the pUC18 derivative, pTZ18R, the S^{21} gene appeared to be the functional equivalent of S^{λ} (Bonovich and Young, 1991). However, the observed lysis was not complete even after an hour from its onset, despite the fact that the S^{21} protein was probably produced at supra-physiological concentrations from the very high copy number plasmid. For this reason, we repeated these experiments with various alleles of $S^{21}68$ and R^{21} expressed from the λ late promoter on a medium copy number plasmid. This system was shown in other work to support lysis with approximately normal timing (Barenboim *et al.*, 1999; Gründling *et al.*, 2000b). As can be seen in Figure 16A, expression of R^{21} from the plasmid complemented the lysis defect of an induced λ*SRam* lysogen, with lysis beginning 55 min after induction and completing within 10 min. In contrast, expression of S^{21} did not complement an induced λ*SamR*

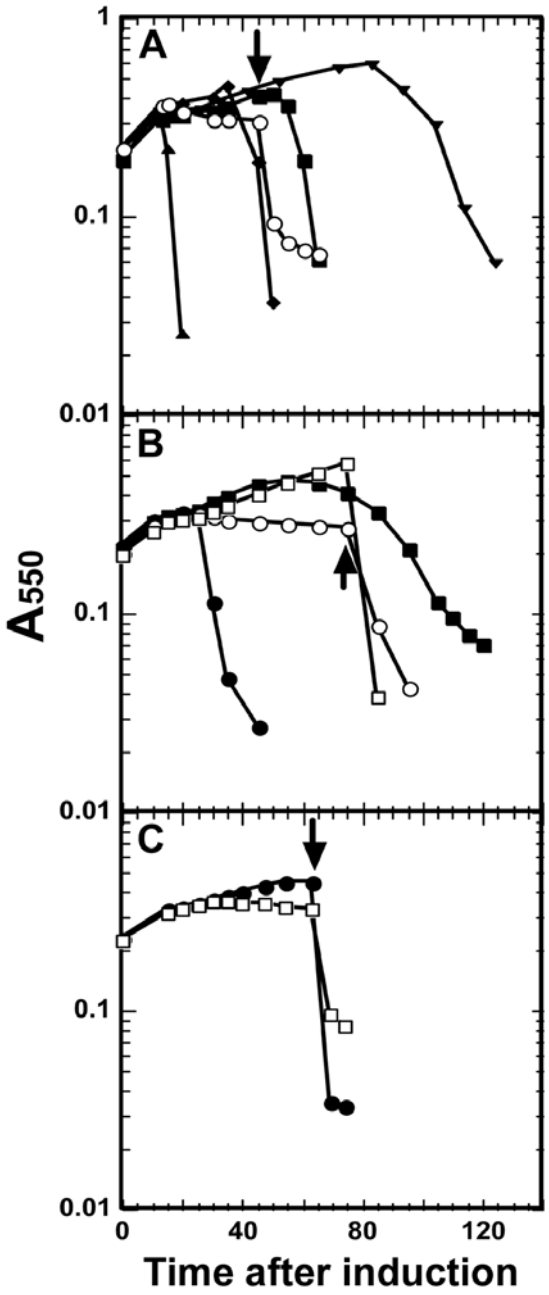

Figure 16. In panel A, lysogens of MC4100 bearing plasmid carrying each indicated alleles were grown and thermally induced. In panel B and C, lysogens of MDS12 *tonA::Tn10* bearing plasmid carrying each indicated alleles were induced thermally and also by addition of IPTG (*Materials and Methods*). A. $S^{21}68$ and S^{λ} are not functionally equivalent. (▲), λ*Δ(SR)*, $S^{21}68R^{21}$; (◆), λ*Δ(SR)*, $S^{\lambda}R^{\lambda}$; (○), λ$S_{am}7R$, $S^{21}68R^{21}{}_{am}$; (■), λSR_{am}, $S^{21}68amR^{21}$; (▼), λ*Δ(SR)*, $S^{21}68amR^{21}$. B. $S^{21}68$ is sufficient for an abrupt lysis phenotype of SAR endolysin of P1 lyz . $CHCl_3$ was added (arrow) to two cultures (○,□) at 75 minutes after induction. (●), λ$S^{21}68R^{21}{}_{am}$, *lyz*; (○), λ$S^{21}68R^{21}{}_{am}$, R^{λ}; (■), λ*Δ(SR)*, *lyz*; (□), λ*Δ(SR)*, R^{λ}. C. $S^{21}68$ is not sufficient for inducing lysis by T4 E. $CHCl_3$ was added (arrow) to both cultures (●,□) at 65 minutes after induction. (●), λ*Δ(SR)*, T4 *E*; (□), λ$S^{21}68R^{21}{}_{am}$, T4 *E.*

lysogen. This was despite the fact that both the S^{21} holin and the λ endolysin were present in lethal quantities in this induced culture, since cell growth stopped at approximately 15 minutes after induction, consistent with the triggering of the holin, and the addition of $CHCl_3$ resulted in immediate lysis, indicating the presence of a pool of cytoplasmic endolysin. Similarly, unlike S^{λ}, S^{21}68 was unable to promote the release of E, the cytosolic endolysin from phage T4. However, co-expression of *lyz*, encoding the SAR endolysin from phage P1, and *S^{21}68* resulted in saltatory and rapid lysis of the host, a characteristic of holin-triggered lysis (Figure 16B). This S^{21}68-facilitated lysis was easily distinguished from the delayed and gradual lysis that occurs when *lyz* is induced in the absence of a holin. Thus, while the phage λ holin, S^{λ}, functions with either a cytoplasmic or a SAR endolysin to achieve host lysis, the phage 21 holin, S^{21}, can cause lysis only when paired with SAR endolysins. This indicates that when S^{21} triggers, it eliminates the membrane potential, thus causing release and activation of the membrane-tethered inactive SAR endolysin, but does not form holes in the membrane large enough to allow passage of a pre-folded, active cytoplasmic endolysin.

III.3.3. Macromolecules easily pass through S^{λ} but not S^{21} holes

In order to demonstrate that S^{λ} but not S^{21} allows the non-specific movement of macromolecules across the inner membrane, the genes for either holin were expressed in cells producing the fluorescent periplasmic marker, TorA-GFP-SsrA. The latter protein has the leader peptide and the first eight amino acids of TorA fused to the N-terminus of a green fluorescent protein variant allowing the Tat-specific secretion of the chimera to

the periplasm. The SsrA sequence at its C-terminus promotes the degradation by the ATP-dependent proteases ClpAP and ClpXP of any of the chimeric protein that escapes export and remains in the cytoplasm. When examined by fluorescence microscopy, a thin ring of fluorescence at the periphery of cells expressing the *TorA-GFP-SsrA* gene is observed (Figure 17A) indicative of the periplasmic localization of the TorA-GFP-SsrA protein. The induction and triggering of S^{λ} results in cells with periplasmic TorA-GFP-SsrA results in a uniform, diffuse fluorescence throughout the cytoplasm (Figure 17B). Lack of degradation of the fluorescent chimera by ClpAP and ClpXP is due to the rapid

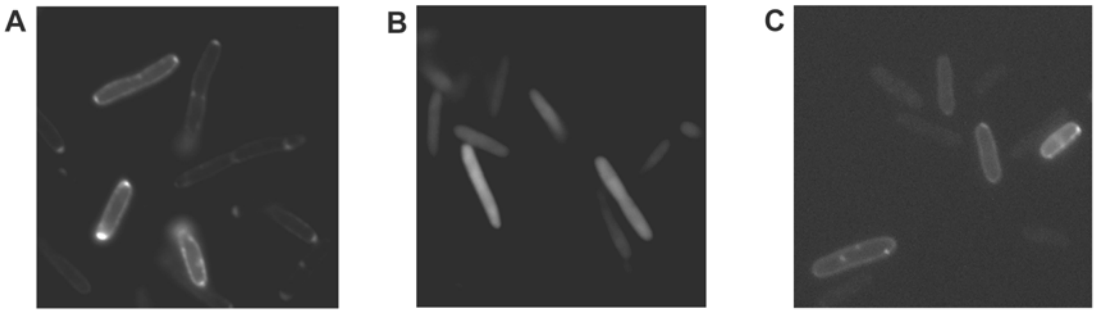

Figure 17. Holin-specific localization of GFP implies differences between S105 and $S^{21}68$ hole formation. In all panels, MDS12 *tonA::Tn10* $\lambda\Delta(SR)$ lysogens bearing pTGS and each indicated plasmid carrying S105 or $S^{21}68$. Cells were grown, induced, and examined as described in Materials and Methods. A. vector control. B. S105. C. $S^{21}68$.

depletion of ATP subsequent to the formation of S^{λ} holes in the inner membrane. By contrast, the induction and triggering of S^{21} in cells with periplasmic TorA-GFP-SsrA did not cause its redistribution to the cytoplasm (Figure 17C).

III.3.4 Genomic analysis of type II holins with SAR endolysin

S^{21} is a class II holin, with two TMDs and an initial N-in, C-in topology. In Chapter II, it was shown that TMD1 of S21 has SAR-domain character, in that it exits the bilayer during the pathway to hole formation. Moreover, previous results from this laboratory demonstrated that the phage 21 endolysin is a SAR endolysin; its N-terminal TMD exits the bilayer, which releases the endolysin into the periplasm and also results in its activation (Xu *et al.*, 2004). It was of interest to see if the presence of a SAR endolysin is associated with SAR-TMD1 holins in other phage lysis cassettes. In order to test our hypothesis, the genomic sequences of Gram-negative bacteriophages carrying the genes for the SAR endolysins were screened for existence of class II holin genes. Sixty-four sequences were identified and aligned. The alignment (Figure 18) shows clearly that there are multiple different gene families of class II holins. Although the S^{21} family is the largest, with 29 members, there are 8 other families with 2 or more members, and 13 unique sequences. A single representative of most of the families was used for further analysis.

To determine whether each candidate class II holin had a TMD1 with SAR character, a method for screening the amino acid sequences was needed. As shown previously with P1 Lyz, R^{21}, and TMD1 of S^{21}68, one of the common characteristics of the SAR domain is that it is rich in weakly hydrophobic residues, such as Gly, Ala, Thr, and Ser. A reliable hydrophobicity scale for amino acid residues has been developed by Deber and colleagues, based on reverse-phase HPLC retention times of model peptides (Deber *et al.*, 1999). Using the Deber scale, a SAR index, or running sum of

hydrophobicities, was calculated for each position of each TMD1, using the following formula:

Equation 1 $\sum_{i=1}^{N} H_i = H_1 + H_2 + \ldots + H_N$ = running sum of the hydrophobicities of residues 1 to N, where H_i = hydrophobicity of residue i in a sequence of N residues

The SAR index was plotted versus residue number for each TMD1 sequence (Figure 19). A standard for a TMD which had no SAR character was needed. In an effort to design α-helices that insert spontaneously into membranes as TMDs, Wimley and White engineered the TMX-1 peptide, which is a 31-residue sequence with a 21-residue nonpolar core (Wimley and White, 2000). Using TMX-1 as the "non-SAR" standard, the TMD1s from the class II holin collection were classified as 1. above TMX-1: TMD, 2. proximal but below TMX-1: possible SAR, 3. far below TMX-1: likely SAR. The results are shown in Table 3. Clearly there is no requirement that the SAR endolysin be associated with a holin equipped with a SAR-like TMD1.

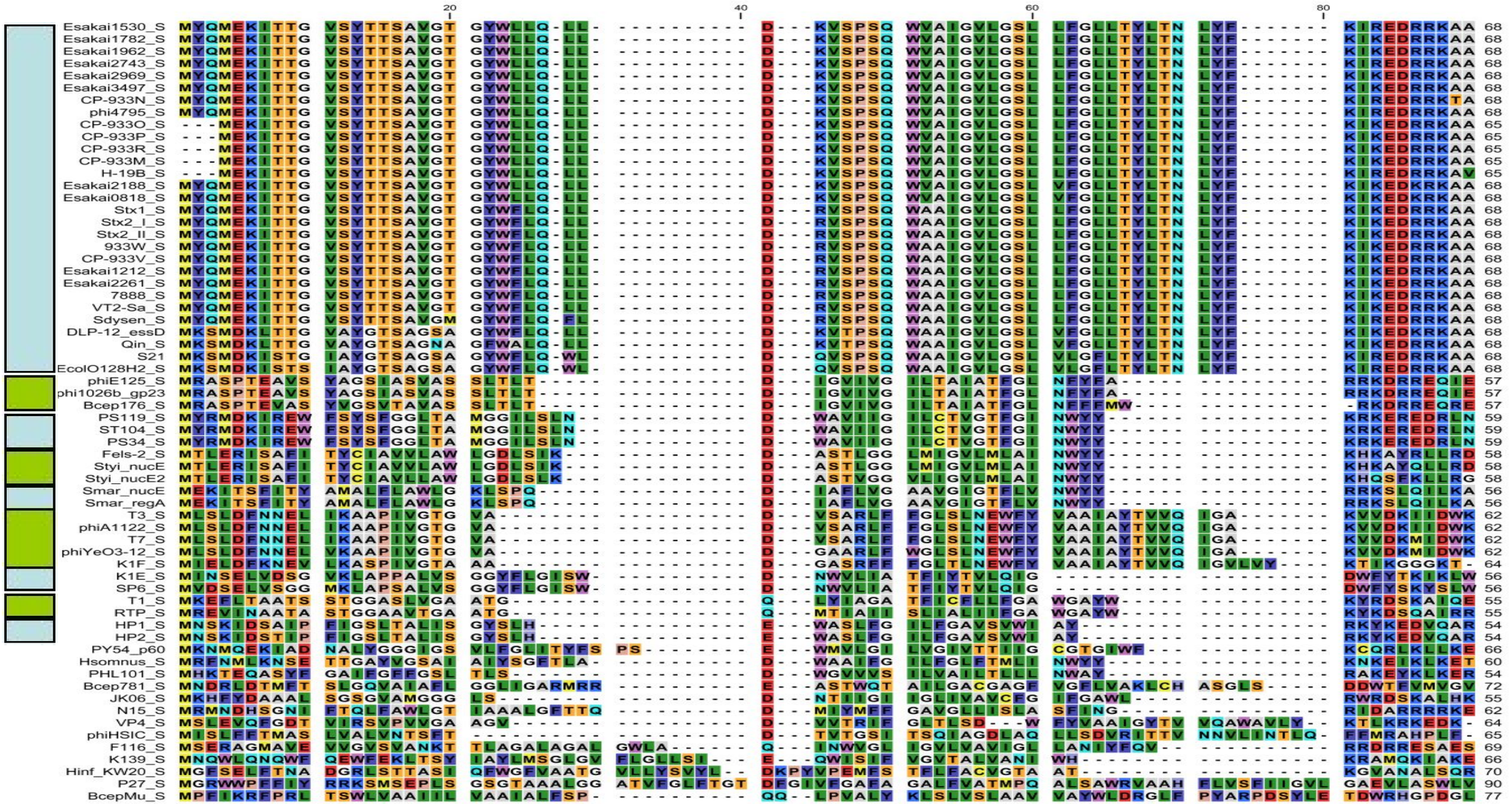

Figure 18. Alignment of type II holins. Alignment strategy was to align the two TMDs independently, surrounding a central negatively-charged or hydrophilic residue, assumed to be in the periplasmic loop. The highly charged C-terminal domain starts at consensus position 81, with the exception of the two holins, P27 and BcepMu, at the bottom. To the left are boxes showing the multi-member groups of related holins. The largest group is the S21 family, at the top. 13 holins at the bottom of the alignment are unique sequences, with no related holins.

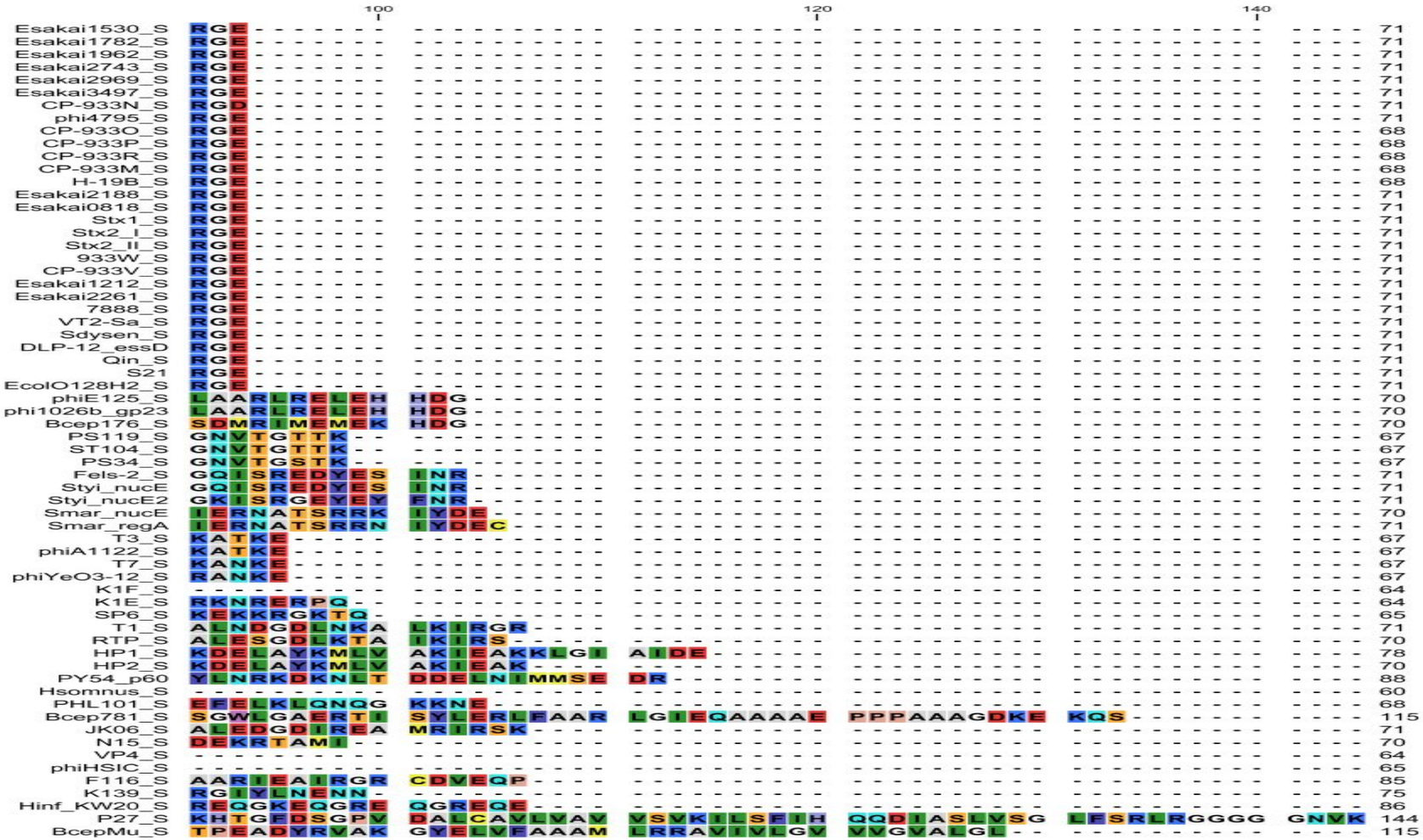

Figure 18. Continued.

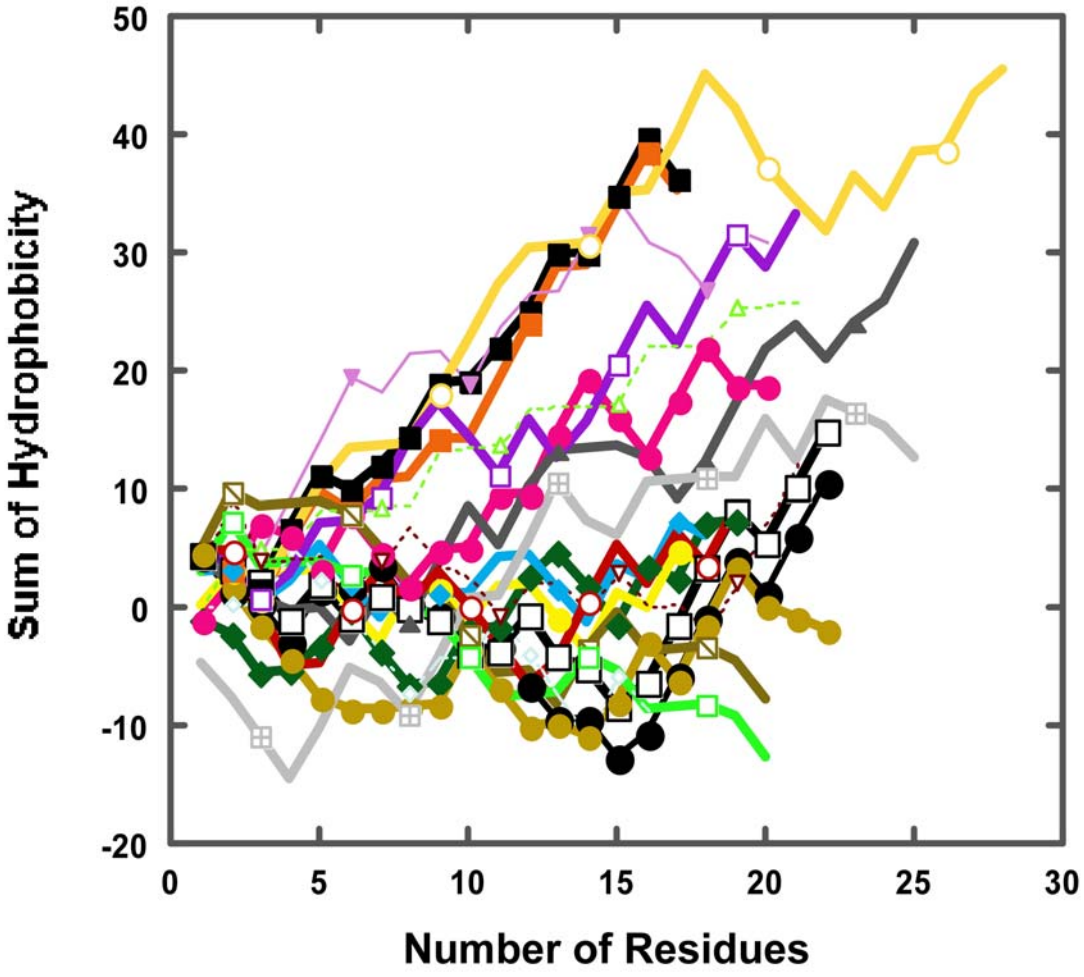

Figure 19. Sum of hydrophobicity plot based on the "SAR index". Sum of hydrophobicity was plotted versus number of residues in the TM α-helices. (●), S^{21}; (black □), Stx1; (green ◆), Hsomnus; (■), Fels-2;(pink ●), Bcep781; (gold ●), P27;(yellow ●), phiE125; (orange ■), Smar nucE;(blue ◆), Bcep176; (gray ▲), KW20;(▼), phiHSIC; (yellow ○), BcepMu; (▨), T1; (gray □), N15; (green □), RTP; (○), K1E; (violet □), K139; (◇), JK06; (△), TMX-1 peptide.

Table 3. The presence of SAR endolysin does not necessarily correlate with the presence of SAR holin. *Hsomnus*, *Hemophilus somnus*; *Smar*, *Serratia marcescens*.

Source of holin	Presence of SAR Holin	Presence of SAR Endolysin
Phage 21	Yes	Yes
Stx1 converting phage 1	Yes	Yes
Hsomnus phage	Yes	Yes
P27	Yes	No
phiE125	Yes	No
Bcep176	Yes	Yes
T1	Yes	Yes
RTP	Yes	Yes
K1E	Yes	No
JK06	Yes	Yes
N15	Yes	Yes
T7	Possible	No
Bcep781	Possible	No
KW20	Possible	No
BcepMu	No	No
Fels-2	No	Yes
Smar phage	No	Yes
phiHSIC	No	No
K139	No	Yes

III.4. Discussion

III.4.1. Role of S^{21} in the regulation of R^{21}.

When a cytoplasmic endolysin, such as R^{λ} and T4 E, was provided *in trans*, expression of the holin $S^{21}68$ caused cessation of growth but was not able to bring about host lysis (Figure 16), despite the fact that there was an accumulation of sufficient endolysin in the cytoplasm. However, when the SAR endolysin P1 Lyz was provided *in trans* to $S^{21}68$, host lysis was obtained. These results point out two characteristic features of S^{21} in host lysis: (a) when S^{21} triggers, it collapses the membrane potential, thus causing release and activation of the membrane-tethered inactive SAR endolysin, but does not form holes in the membrane large enough to allow passage of a pre-folded, active cytoplasmic endolysin, (b) the $S^{21}68$ triggering is not R^{21} specific, since it occurs with a heterologous cytoplasmic endolysin (Figure 16).

Previously, there have been three holins studied in detail: S^{λ}, T4 T, and PRD1 p35 (Raab *et al.*, 1986; Ramanculov and Young, 2001b; Rydman and Bamford, 2003). For all of these, it has been proposed that the critical functions were (a) permeabilization of the membrane to allow escape of the endolysin and (b) timing of the length of the vegetative phage. That is, mutants could be isolated that were defective either in hole-formation or in the timing of hole formation (i.e., too early), which would abolish the function of the holin. However, to bring about host lysis, $S^{21}68$, must be provided with the SAR endolysin which does not depend on the holin for transit to the periplasm. Thus the S^{21} holin appears to have only a timing function.

One question which could be asked is why have a holin at all if the phage has a SAR endolysin? Indeed, here we demonstrate that a phage carrying a null mutation in the S^{21} holin does not lose plaque-forming ability (Figure 15). Nevertheless, the phage plaque morphology and lysis physiology in the present and absence of holin function was revealing. From the plating test, λ $S^{21}68R^{21}$ formed large plaques of uniform size on non-suppressor hosts (Figure 15A). Moreover, in liquid culture, the lysis of induced λ $S^{21}68R^{21}$ lysogens displayed a saltatory nature, indicative of its holin-mediated timing. The behavior of λ $S^{21}68_{am}R^{21}$ was different with respect to both phenotypes. While λ $S^{21}68_{am}R^{21}$ was a plaque former, the plaques were small and showed a considerable size variation (Figure 15B). When phages from large and small plaques were replated, this heterogeneity still persisted (Figure 15C). When λ $S^{21}68_{am}R^{21}$ was induced in liquid culture, the lysis time was delayed and gradual, indicating a wide variation in the time that the individual induced cells undergo lysis. These observations suggest that although non-essential by the strict definition of being required for plaque formation, the S^{21} holin provides an important lysis timing function. The small, variable plaque size presumably reflects variability in the individual rounds of growth that go on during the formation of the plaque. Theoretical analysis has indicated that, for any host, host density, and environmental condition, there should be an ideal time of lysis that will maximize viral titer (Wang *et al.*, 1996). The holin, whether it is a holin that releases cytoplasmic endolysin or merely triggers to activate a tethered SAR endolysin, provides a more uniform lysis timing for each infection cycle. This should accelerate evolutionary adjustments to timing that may be required to accommodate changed culture conditions.

III.4.2. Holin vs. pinholin

From the fact that $S^{21}68$ is permissive for P1 Lyz, but not for R^{λ} and T4 E, we hypothesize that the S^{21} holin makes holes too small to allow the passage of R^{λ} from the cytoplasm to the periplasm. In order to test our hypothesis, we performed a localization experiment of the fluorescent periplasmic marker, TorA-GFP-SsrA. When the TorA-GFP-SsrA fusion protein was expressed with $S^{21}68$, a thin ring of fluorescence at the periphery of cells is observed by fluorescence microscopy (Figure 17A). This peripheral ring indicates the periplasmic localization of the TorA-GFP-SsrA protein. On the other hand, the induction and triggering of S^{λ} results in cells with periplasmic TorA-GFP-SsrA results in a uniform, diffuse fluorescence throughout the cytoplasm (Figure 17B). We interpret these results such that, unlike S^{λ}, $S^{21}68$ forms a "pinhole"; thus macromolecules easily pass through S^{λ} holes but not S^{21} holes. This result again supports our interpretation: when S^{21} triggers, it only needs to collapse the membrane potential, thus causing release and activation of the membrane-tethered inactive SAR endolysin, but does not form holes in the membrane large enough to allow passage of a pre-folded, active cytoplasmic endolysin.

III.4.3. Implications for the evolution of holin-endolysin systems

At physiological levels of expression, the S^{21} holin makes holes too small to allow the passage of R^{λ} from the cytoplasm to the periplasm. We propose that holins of this type to be called "pinholins" to suggest their small hole size. We think that the

S^{21}/R^{21} gene pair may represent an intermediate stage in the evolution of holin-endolysin systems. The most primitive of such lysis systems probably consisted only of a SAR endolysin. This system would provide a lysis delay because of the gradual release and activation of the membrane-tethered endolysins, and, due to their sensitivity to membrane depolarization, would provide a sentinel function to effect emergency lysis in the event of super-infection. However, a lysis system employing a SAR endolysin alone would be inherently leaky, difficult to control, and not as saltatory as the more modern holin-endolysin system of phage λ. The subsequent acquisition of a depolarizing holin would correct the latter two weaknesses. Further optimization would involve first, alterations in the holin that would allow it to form protein-sized membrane lesions and, second, loss of the N-terminal SAR domain from the endolysin. In this more evolved system, lysis is absolutely holin-dependent since the endolysin is restricted to the cytoplasmic compartment until holin triggering.

III.4.4. Class II holins with SAR-TMD1s are common but are not correlated with SAR endolysins

$S^{21}68$ has two striking features: it is a pinholin, contributing to lysis only by forming a small hole in the membrane to collapse the proton-motive-force, and it has a SAR-like TMD1 which must exit the bilayer during the hole-formation pathway. Since the exit of TMD1 was shown to be a part of lethal action of $S^{21}68$ and only TMD2 is required for hole formation, we wondered if all phages containing SAR endolysin might carry a "SAR holin"; i.e., a class-II holin with a SAR-like TMD1, or vice-versa.

Furthermore, it was of interest to see if the SAR holins were all related to S^{21}. A large number of class II holins were found in the database. Analysis of the alignments clearly demonstrate that, although about half of the sequences are members of the S^{21} family, there are multiple unrelated families in this group (Figure 18). Moreover, using the SAR index developed for this analysis, it was shown that of the class II holin families collected from the database, about half have clearly identifiable SAR-like TMD1s (Figure 19; Table 3). However, a considerable number also have TMD1s with normal hydrophobicity. Thus there is nothing essential about the exit of TMD1 in class II holins. What is also clear is that some class II holins are not associated with SAR endolysins. The best example is the holin from phage T7, gp*17.5* (entered as T7_S in Figure 18). The endolysin of phage T7 is gp*3.5*, a cytoplasmic amidase (Inouye *et al.*, 1973); thus, the T7 class II holin cannot be a pinholin. That is, there is nothing about being a class II holin that prevents large hole formation. The most interesting conclusion from the bioinformatic analysis is that some SAR-endolysins are able to function with cytoplasmic endolysins (e.g., the holin of phiE125). This indicates that there is nothing about the exit of TMD1 from the bilayer that forces a class II holin to make only a "pinhole". In other words, a single TMD in the bilayer is all that is required for large hole formation.

CHAPTER IV

MUTATIONAL ANALYSIS OF THE *S*^{21}*68* GENE

IV.1 Introduction

Holins are small, phage-encoded membrane proteins that work in conjunction with an endolysin to bring about host lysis at the end of the infectious cycle. For all endolysins lacking secretory signals, the holin must create lesions in the cytoplasmic membrane that are of sufficient size to allow movement of the endolysis from the cytoplasm to the periplasm (Young, 1992; Young *et al.*, 2000). In the cases where an inactive form of the endolysin is secreted by the *sec* system, the holin needs only to depolarize the cytoplasmic membrane in order for endolysin activation to occur (Xu *et al.*, 2004; Young *et al.*, 2000).

It is generally accepted that holins must oligomerize in order to permeabilize the cytoplasmic membrane. To define the oligomerization pathway and to identify specific contacts made between holin TMD(s), three different holins have been subjected to mutational analysis. In the first such study, a large collection of lysis-defective, mutants in *S*$^{\lambda}$ was generated by hydroxylamine mutagenesis. Within this collection were defective alleles with mutations 5' to the coding sequence and their existence lead to the discovery of the dual-start motif of *S*$^{\lambda}$ and the S$^{\lambda}$ antiholin. This collection also contained many missense alleles that were partially dominant when co-expressed with the wild type providing the first evidence, albeit indirect, that S$^{\lambda}$ oligomerizes in the membrane. In subsequent studies, chemical crosslinking demonstrated that S$^{\lambda}$ exists as

monomers, dimers, and higher oligomers in the cytoplasmic membrane. The fact that certain lysis defective alleles were blocked at the monomeric, dimeric, or oligomeric states was instrumental in developing the model for S^{λ} function that is shown in chapter I (Figure 6). Many additional missense alleles of S^{λ} have been obtained since the initial collection was generated. The most surprising finding to result from this work was that the "triggering time" of S^{λ} could be affected dramatically in either direction by changes at any position in its three TMDs. Moreover, the effect on triggering time was completely unpredictable. For example, in an exhaustive analysis of missense mutations at position 52 in TMD2, it was found that triggering could be greatly accelerated by the A52F or A52G substitutions and it could be delayed or abolished by the A52Y or A52V substitutions (R. White, personal communication).

A less extensive genetic analysis of the type I holin (gp35) from phage PRD1 has been reported (Rydman and Bamford, 2003). Missense mutations that accelerated (W67S, W67Q, and W77C) or delayed lysis (W8S, W8Q, W8Y, W67Y, and D81Y) were found in TMD1 and TMD3. In addition, six insertional mutants, generated with mini-Mu in vitro transposition technology, were found to exhibit a delayed lysis phenotype (Rydman and Bamford, 2003; Vilen *et al.*, 2003). These mini-Mu insertions were localized to the 3' end of gene *35* suggesting that the charged C-terminus of gp35 is involved in the timing of host lysis.

A preliminary analysis of a collection of mutant alleles of the class III holin, T, from bacteriophage T4 arising spontaneously or through UV irradiation has been reported (Ramanculov and Young, 2001). In contrast to what was found with S^{λ}, nearly

all of the lysis timing (triggering) mutants were found in the C-terminal periplasmic domain and not in the predicted TMD. Instead, mutations in the TMD seemed to affect the rate at which lysis was observed in the bulk culture. While the significance of this has not been further investigated, these slowly-lysing mutants might reflect a partial defect in the ability to form holes large enough to allow the release of endolysin from the cytoplasm to the periplasm after the triggering event has occurred. Finally, as would be expected from the studies of Tran et al. (Tran *et al.*, 2005) mutations which affected the phenomenon called lysis inhibition (LIN) were found to reside exclusively in the periplasmic domain of T.

The lysis region of lambdoid bacteriophage 21 consists four genes, *(SRRzRz1)*^{21} (Figure 20). The holin from phage 21, S^{21}, is a class II holin having two predicted transmembrane helices (Bonovich and Young, 1991; Barenboim *et al.*, 1999; Young and Bläsi, 1995). Like most holin genes of lambdoid phages, the *S* gene of phage 21 has a "dual-start motif" that controls the ratio between the holin (S^{21}68) and antiholin (S^{21}71) forms of S^{21} (Bonovich and Young, 1991; Barenboim *et al.*, 1999). S^{21}71 is identical to S^{21}68 except for the N-terminal sequence Met-Lys-Ser.., which provides an additional positive charge when compared to the N-terminus of S^{21}68. We have recently reported that the predicted TMD1 of S^{21} is a SAR domain that can exist as either a TMD or in the aqueous phase. Moreover, when in the membrane, TMD1 prevents hole formation by TMD2 while specific TMD1-TMD1 interactions facilitate hole formation when it is in the aqueous phase (periplasm).

A.

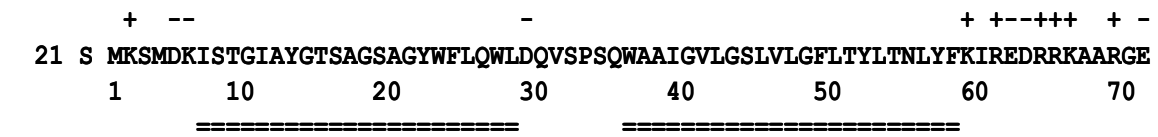

B.

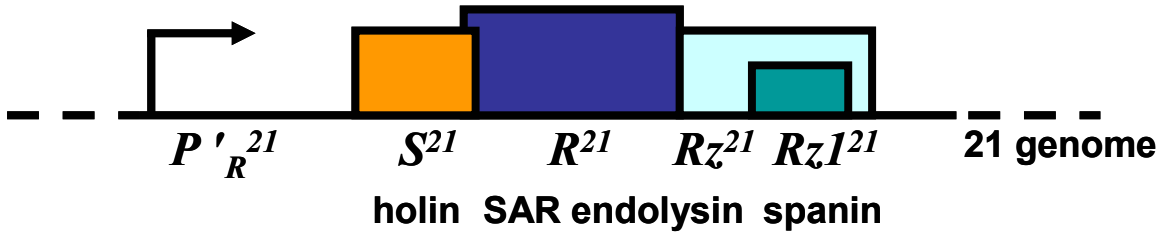

Figure 20. A. Primary structure of the S^{21} holin. Charged residues are indicated above the sequence. Putative transmembrane domains are underscored with the symbol (= =). B. Lysis cassettes of phage 21. The lysis genes of phage 21 are shown, along with their late gene promoters.

While no class II holin has been subjected to a thorough genetic analysis as of yet, S^{21} is an attractive candidate since the two TMDs of S^{21} have distinct roles in programmed cell lysis. Here, I report preliminary findings from the first mutational analysis performed with $S^{21}68$.

IV.2. Materials and methods

IV.2.1. Bacterial strains and culture conditions

All bacterial cultures were grown in standard LB medium, supplemented with various antibiotics when appropriate: ampicillin, 100 μg/ml; rifampicin, 100 μg/ml; kanamycin, 40μg/ml; and tetracycline, 10 μg/ml. When indicated, isopropyl β-D-thiogalactoside (IPTG), arabinose, or $CHCl_3$ were added at final concentration of 1mM, 0.2 %, or 1%, respectively.

Standard conditions for the growth of cultures and the monitoring of lysis kinetics have been described (Chang *et al.*, 1995; Smith and Young, 1998). Ethylmethane sulfonate (EMS) mutagenesis was performed with XL1-Blue cells (Smith *et al.*, 1998b). All other experiments were done with a *lacI*^{q1} *tonA::*Tn*10* derivative of MG1655, the sequenced wild-type strain of *E. coli* K-12 (Guyer *et al.*, 1981).

IV.2.2. Standard DNA manipulation, PCR, and DNA sequencing

Procedures for the isolation of plasmid DNA, DNA amplification by PCR, PCR product purification, DNA transformation, and DNA sequencing have been described (Smith *et al.*, 1998a; Smith *et al.*, 1998a; Gründling *et al.*, 2000). Oligonucleotides were

obtained from Integrated DNA Technologies, Coralville, IA, and were used without further purification. Ligation reactions were performed by using the Rapid DNA ligation kit from Roche Molecular Biochemicals according to the manufacturer's instructions. All other enzymes were purchased from Promega, with the exception of *Pfu* polymerase, which was from Stratagene. Automated fluorescent sequencing was performed at the Laboratory for Plant Genomic Technologies in the Crop Biotechnology Center at Texas A&M University.

IV.2.3. Plasmids and induction

For most experiments, the bacterial strains carried two plasmids, a low copy plasmid pQ, carrying the gene for the λ late gene activator, Q, under $P_{lac/ara-1}$ control , and a medium copy plasmid with a pBR322 origin and a hybrid lysis cassette consisting of $S^{21}68(RRzRz1)^{\lambda}$. The later plasmid was generated using the scheme shown in Figure 21. Induction of the lysis genes was accomplished by adding 1 mM IPTG and 0.2% arabinose to the culture. The lysis gene cassettes were either from λ or phage 21, as indicated.

IV.2.4. SDS/PAGE and Western blotting

Cell culture aliquots were adjusted to 10% TCA and placed on ice for 30 minutes. The precipitate was collected by centrifugation and washed with acetone to remove the TCA. Pellets were air-dried and resuspended in SDS-PAGE loading buffer. SDS/PAGE and Western blotting were performed as described (Gründling *et al.*, 2000). Antisera

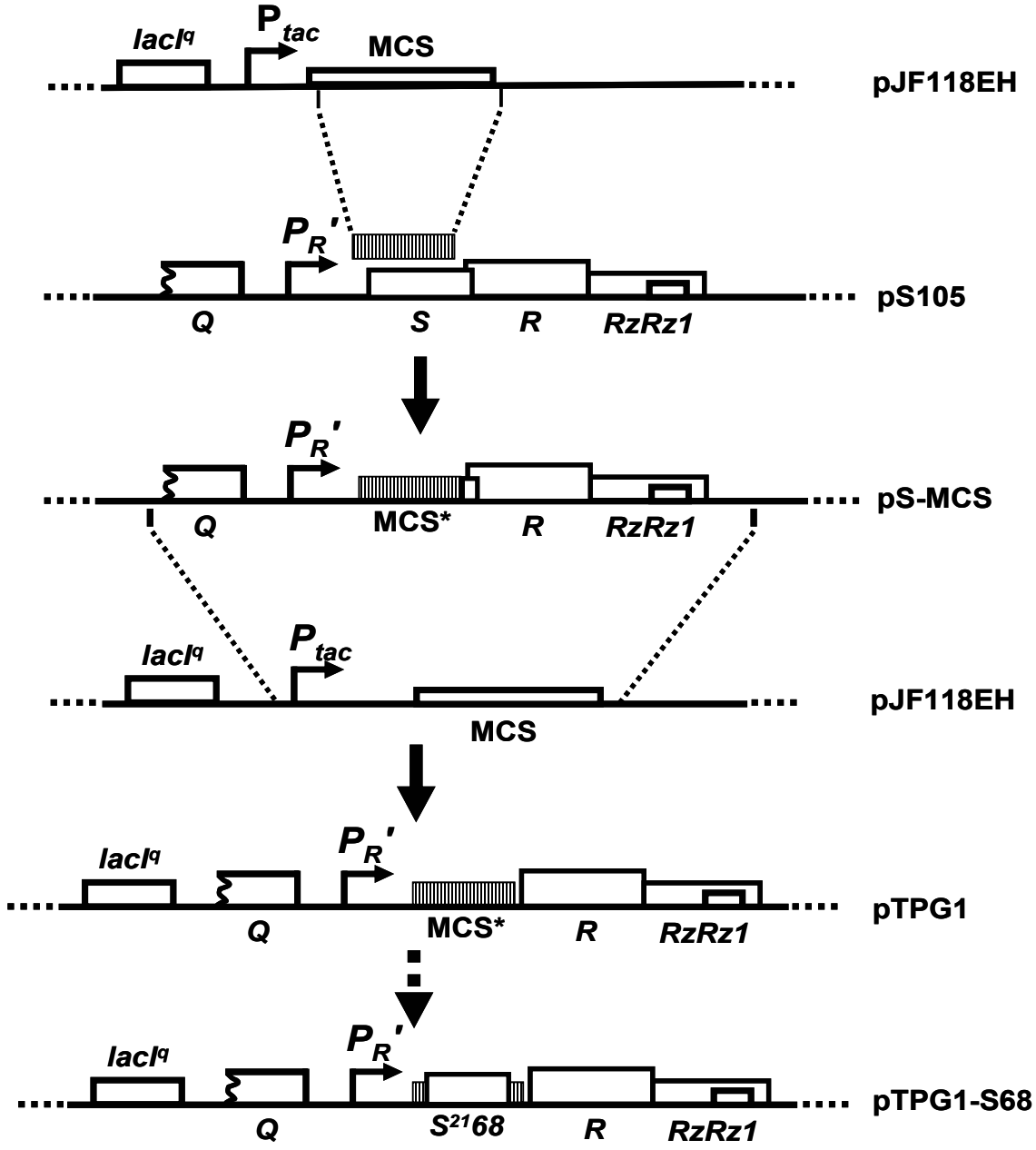

Figure 21. Construction of pTPG1-S68 containing the hybrid lysis cassette, $S^{21}68(RRzRz1)^{\lambda}$. Briefly, the S^{λ} gene of pS105 ($S^{\lambda}R^{\lambda}Rz^{\lambda}Rz1^{\lambda}$) was replaced with the multiple cloning site (MCS) from pJF118EH forming pS-MCS. Next, the entire lysis region of pS-MCS, including the promoter, was used to replace the promoter and MCS of pJF118EH yielding pTPG1. Finally, the $S^{21}68$ gene and its upstream Shine-Dalgarno sequence was inserted into the MCS of pTPG1 generating pTPG1-68.

against the peptide KIREDRRKAARGE, which corresponds to the S^{21} C-terminus, was raised in rabbits (Barenboim *et al.*, 1999). Horseradish peroxidase-conjugated secondary antibodies against rabbit IgG were from Pierce. Generally, primary antibodies were used at a 1:1000 dilution, whereas secondary antibodies were used at a 1:3000 dilution. Blots were developed by using the chromogenic substrate 4-chloro-1-naphthol.

IV.2.5. EMS mutagenesis of pTPG1-S68

EMS mutagenesis was performed by the procedure of Miller (Miller, 1992) using the *recA*- strain XL1-blue carrying monomeric pTPG1-S68. After exposure to EMS, cells were washed and plated on LB agar to measure cell viability. The degree of mutagenesis was estimated by outgrowth of the EMS-treated cells followed by plating of LB agar containing rifampicin as described by Miller (Miller, 1992).

IV.2.6. Screen for S68 lysis defective mutants

After overnight growth of the EMS-treated cells, plasmid DNA was recovered and transformed into the host, MG1655 *lacI*^{q}, which also carried the pQ plasmid. A portion of the transformant pool was inoculated into 25 ml LB medium and the culture was grown to an A_{550} of 0.2 and then induced with addition of IPTG and arabinose for 2hrs. After the induction, cells were collected by centrifugation and plated on LB agar without inducer. Surviving colonies were inoculated individually into LB medium, induced at A_{550} of 0.2, grown for 2 hours and then exposed to $CHCl_3$. Cultures that lost their turbidity after the addition of $CHCl_3$ were presumed to have produced R^{λ} and were

likely to harbor a lysis-defective *S21 68* allele. The pTPG1-S68 plasmid was recovered from these cultures and was re-transformed to fresh MG1655 *lacI*^{q} cells to confirm that the lysis defective phenotype segregated with the plasmid. All the candidate plasmids that passed this final test confirmation were subjected to DNA sequence analysis.

IV.3. Results

IV.3.1. Mutational analysis of $S^{21}68$

In order to obtain a pool of lysis-defective alleles of *S21 68*, the *S21 68*$^+$ *R*$^{\lambda+}$ plasmid, pTPG1-S68, was constructed. This plasmid has several features to facilitate the isolation of *S21 68* mutants. First, the Shine-Dalgarno sequence was strengthened to increase the amount of $S^{21}68$ produced after induction. Second, the *R21* gene of the phage 21 lysis cassette was replaced by *R*$^{\lambda}$. Unlike R^{21}, R^{λ} is not deleterious to the host cells. The presence of the *R*$^{\lambda}$ gene immediately downstream of *S21 68* provides a reporter for transcription of the hybrid lysis cassette of pTPG1-S68. Cells producing R^{λ} rapidly lyse after the addition of $CHCl_3$ allowing for the facile elimination of all mutants that severely affect expression of the genes contained in the lysis cassette.

EMS causes primarily G/C to A/T transitions (Greene *et al.*, 2003). Thus, based on the known sequence of the *S21 68* gene, we would expect to that our potential pool of *S21 68* lysis-defective alleles would contain, at most, 10 different nonsense mutations and 88 different missense mutations in *S21 68*. Although it is impossible to predict the effect of individual missense mutations on $S^{21}68$ function, it is reasonable to assume that, with one exception, all of the possible nonsense mutations in *S21 68* would be recovered by our

Table 4. $S^{21}68$ lysis-defective alleles recovered after EMS mutagenesis

Codon	Amino acid change	Codon change	Number of independent isolates
15	Thr Ile	ACA ATA	4
16	Ser Phe	TCT TTT	1
23	Trp End	TGG TGA	2
26	Gln End	CAG TAG	1
27	Trp End	TGG TAG	1
27	Trp End	TGG TGA	3
29	Asp Asn	GAT AAT	4
29	Asp Val	GAT GTT	1
30	Gln End	CAG TAG	1
33	Pro Leu	CCG CTG	1
33	Pro Ser	CCG TGA	1
36	Trp End	TGG TAG	1
36	Trp End	TGG TGA	2
37	Ala Val	GCT GTT	1
38	Ala Thr	GCG ACG	3
43	Gly Glu	GGA GAA	4
43	Gly Arg	GGA AGA	1
51	Thr Ile	ACT ATT	5
54	Thr Ile	ACA ATA	1
62	Glu Lys	GAA AAA	1

selection/screen. The one exception is the expected opal mutation at codon 65 which would result in the production of a 61 residue derivative of $S^{21}68$ that might, potentially, retain its lethality. Of the 150 clones that survived induction and still produced sufficient R^{λ} for lysis after the addition of chloroform, 39 had either missense or nonsense mutations in the *S21 68* gene. The other 111 clones were not further analyzed. Our final mutant pool consisted of 7 unique nonsense and 13 unique missense mutations which are described in Table 4. Of the 10 nonsense mutations expected from EMS mutagenesis, 7 were recovered in our selection/screen. Assuming that the $R65_{opal}$ allele is functional, we recovered 7/9 (78%) of the predicted nonsense alleles. When expression of any of the 13 missense alleles was induced, the cultures displayed nearly normal growth for approximately 2 hours after which culture turbidity begins a slow, steady decline (Figure 22). Under the same conditions, the induction of *S21 68* causes growth cessation after about 1 hour after which the culture turbidity remains essentially constant. We interpret the loss of culture turbidity seen after induction of the mutant *S21 68* alleles to be a reflection of the toxicity associated with the overproduction of a membrane protein.

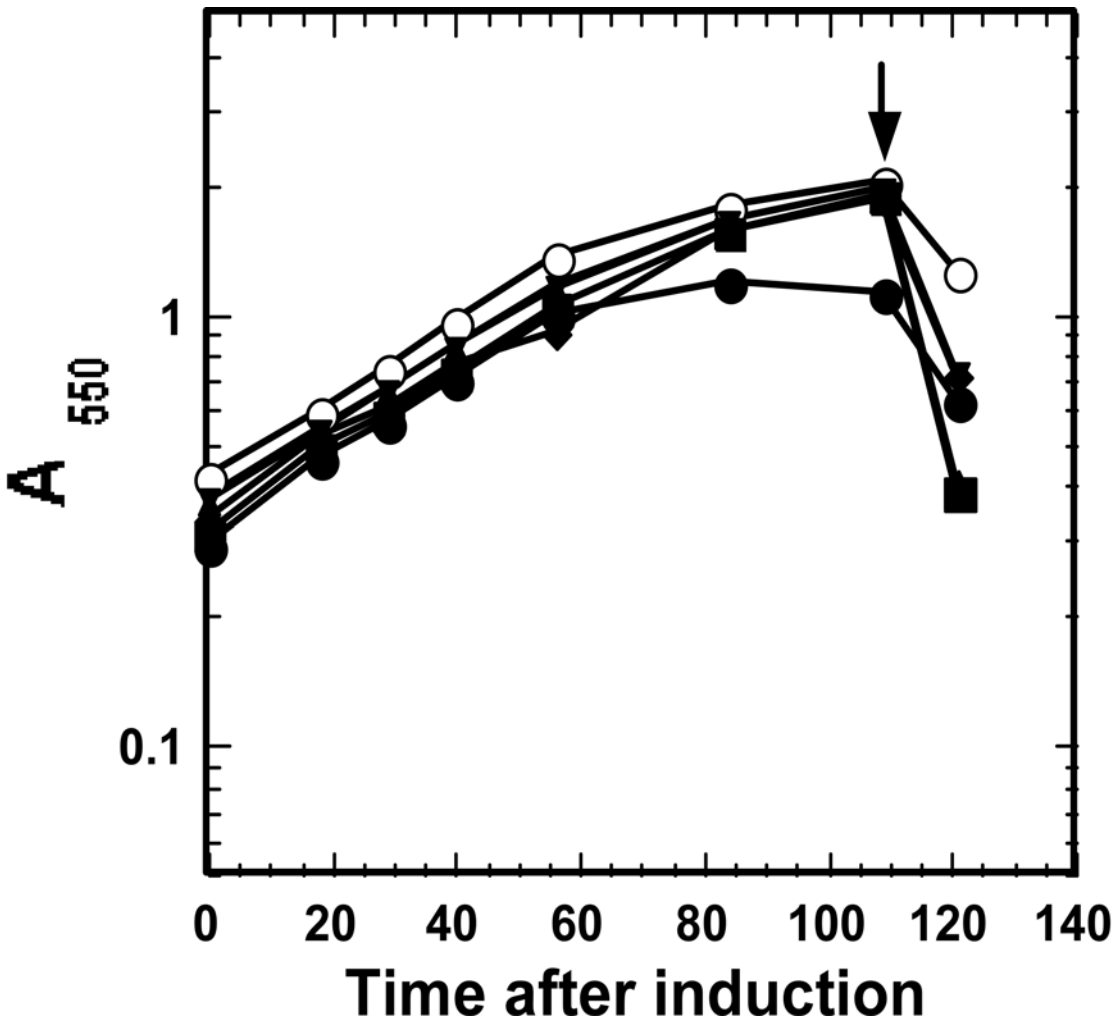

Figure 22. Cells expressing lysis-defective $S^{21}68$ alleles grow past the normal triggering time for $S^{21}68$. Cultures were induced at time zero and culture turbidity was followed as a function of time. The different $S^{21}68$ alleles were carried on pTPG1-S68; (●), *S68*; (■), $S68_{D29N}$; (◆), $S68_{T15I}$; (▼), $S68_{G43E}$; (▲), $S68_{E62K}$. At 110 minutes, $CHCl_3$ was added to each culture (downward arrow) and the immediate drop in turbidity indicates production of R^{λ}.

IV.3.2. Distribution of the mutations in the lysis-defective alleles of *S^{21}68*

The 13 missense mutations recovered (Table 1) were distributed as follows: 2 in TMD1 (T15I, S16F), 4 in the periplasmic loop connecting TMD1 and TMD2 (D29N, D29V, P33L, P33S), 6 in TMD2 (A37V, A38T, G43E, G43R, T51I, T54I), 1 in the C-terminal cytoplasmic domain (E62K). As expected, the majority of the lysis-defective alleles had changes in TMD2, the domain of S^{21}68 that is most strongly implicated in hole formation. The two mutations in the periplasmic loop eliminated a negative charge between TMD1 and TMD2 of S^{21}68 and may have altered the topology of the holin. Most surprising was the isolation of two mutants with missense changes in TMD1. Since we have shown that TMD1 is not necessary for the lethal function of S^{21}68, we suspect these mutations either strengthen the inhibitory TMD1-TMD2 interaction or result in TMD1-TMD1 interactions that interfere with the oligomerization of TMD2s to form functional holes. In any case, the isolation of these mutants was particularly gratifying since, according to our model, their existence would be predicted even though TMD1 does not have a direct role in the formation of holes by S^{21}68.

IV.3.3. Site-directed mutagenesis of the GxxxG motifs in S^{21}68

Both TMDs of S^{21}68 have potential GxxxG (or small-xxx-small) motifs (Figure 23). GxxxG motifs were first noticed by the Engelman group who demonstrated their importance in mediating the interaction of transmembrane (TM) helices of glycophorin A (Senes *et al.*, 2004; Lemmon *et al.*, 1992). The glycines (or other small residues such

as alanine and serine) which align on one surface of a TM helix, allow very close helix-helix permitting extensive interhelical van der Waals interactions (Javadpour *et al.*, 1999; MacKenzie and Engelman, 1998) and facilitating the intimate approach of the polypeptide backbones and the formation of H-bonds between αH atoms and backbone carbonyls (Senes *et al.*, 2000; Senes *et al.*, 2001). Although their importance for the function of $S^{21}68$ is unknown, the GxxxG motifs of $S^{21}68$ might mediate TMD1-TMD2 (inhibitory for lysis) or TMD1-TMD1 and TMD2-TMD2 (facilitatory for lysis) interactions. These motifs are obvious targets for site-directed mutagenesis in any mutational analysis of S^{21}.

Five of the six changes introduced into these motifs had dramatic effects on $S^{21}68$ protein function (Figure 24). Most strikingly, the G14N, S44N, and S44T mutations all significantly reduced the triggering time suggesting that they disrupted important TMD1-TMD2 interactions that would normally serve to retard hole formation. By contrast, the G40L and G48L changes eliminated the lethality of the $S^{21}68$ protein. The sixth change, G14I had no discernable effect on triggering time.

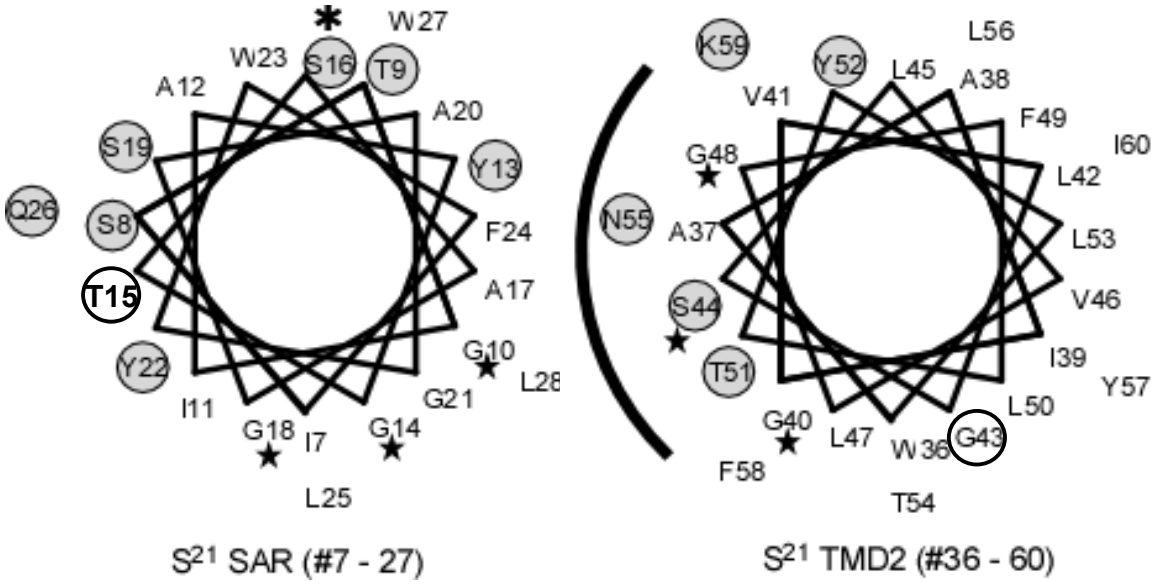

Figure 23. Helical projections of TMDs of S^{21}. Left: the SAR domain (TMD1) of S^{21} (residues 7-27), with the position of the S16C mutation highlighted by an asterisk. Right: TMD2, the hole-forming domain of S^{21} (residues 36-60), with a potential hydrophilic surface that may line the lethal membrane lesion indicated by the arc. Stars indicate GxxxGxxxG-like motifs of each TMD (G10, G14 and G18 in TMD1; G40, S44, G48 in TMD2). Hydrophilic or neutral residues in each TMD are circled and shaded. The empty circles indicate the positions altered for two of the lysis-defective mutants used in the experiment described in figure 24.

IV.4. Discussion

Holins are bacteriophage-encoded proteins with one or more transmembrane helices. The infection cycle is terminated when holin monomers oligomerize in the cytoplasmic membrane forming lesions or holes which allow the movement of water soluble molecules between the cytoplasm and periplasm. It is assumed that the TMDs of the holin proteins line these lesions. The S^{21} protein is one of the smallest holins known and much of its primary structure is predicted to contribute to the formation of two

transmembrane helices or domains. Surprisingly, only one of these TMDs, TMD2, is essential for its lethal, hole-forming function. TMD1 of S^{21} is a SAR domain and exits in both membrane-inserted and periplasmic forms. The presence of TMD1 in the membrane antagonizes hole formation by TMD2. By contrast, when TMD1 enters the

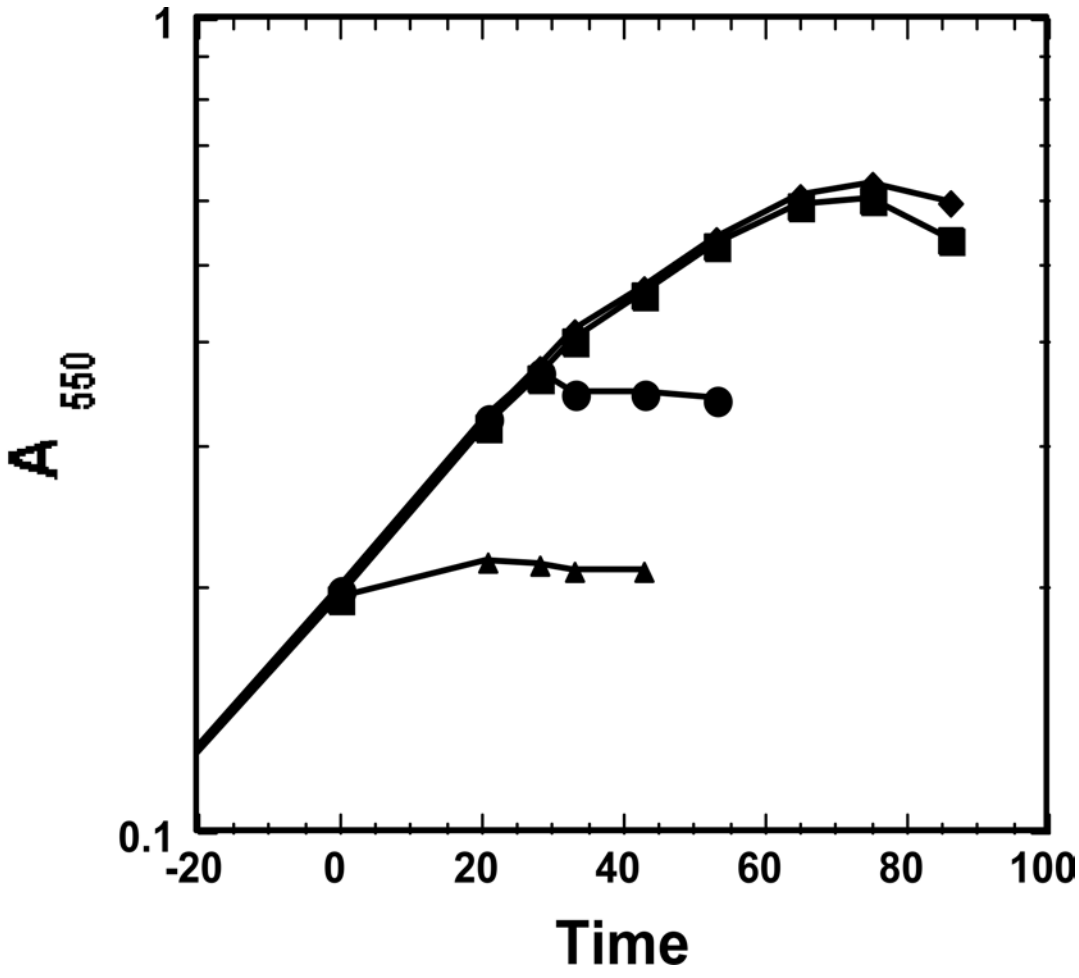

Figure 24. Mutations in the GxxxG motifs can both accelerate and abolish triggering. Cultures were induced at time zero and culture turbidity was followed as a function of time. The different *S*^{21}*68* alleles were carried on pTP2; (●), *S68*; (▲), $S68_{S44T}$; (◆), $S68_{G48L}$; (■), $S68_{G40L}$.

periplasm, TMD1-TMD1 interactions facilitate, but are not required for, S^{21} oligomerization. Based on the roles of TMD1 and TMD2 in hole formation by $S^{21}68$, we would expect to find, at the minimum, two different classes of lysis-defective *$S^{21}68$* alleles. In one class, which I will call "reluctant", the mutation strengthens TMD1-TMD2 interactions preventing the release of the membrane-inserted TMD1 into the periplasm. Thus, a sufficient pool of "free" TMD2 is not available for hole formation. The second class, which I will call "incompetent", the mutation occurs in TMD2 and prevents hole formation by interfering with the process of $S^{21}68$ oligomerization. According to our present understanding of S^{21} function, the two mutations in TMD1 (T15I, S16F) should fall into the "reluctant" class. Evidence supporting this interpretation could be provided by protease shaving experiments of the type discussed in Chapter II. All of the missense mutants in TMD2 that were recovered after EMS mutagenesis presumably represent "incompetent" alleles. This could be directly tested by transferring the mutations to the $S^{21}68_{\Delta TMD1}$ allele. Mutants with altered TMD2-TMD2 interactions would still be defective in this context. Although our anlaysis of the mutants described in this study is incomplete, it is clear that the phenotypes of the mutants we have identified support our contention that TMD1-TMD1, TMD2-TMD2, and TMD1-TMD2 interactions all play a role in hole formation by S^{21} or its timing.

CHAPTER V

CONCLUSIONS

As is the case with all dsDNA phages, bacteriophage 21 encodes two proteins, a holin and an endolysin, that are essential for host lysis and its timing. The function of both of these proteins is under topological control by virtue of SAR domains at their N-termini. SAR domains are recognized as signal-anchor sequences by the *sec* translocon resulting in their insertion into the cytoplasmic membrane. Unlike conventional transmembrane helices which remain membrane-inserted for the life of the protein, SAR domains have the peculiar property of being able to exit the membrane at a measurable rate and adopt a conformation that is compatible with the aqueous phase. Thus, SAR-endolysins are capable of reaching the periplasm as soluble proteins without the assistance of their cognate holins allowing for holin-independent host lysis as was first described for bacteriophage P1. Although the release of SAR-endolysins to the periplasm occurs spontaneously, it is accelerated by the depolarization of the cytoplasmic membrane. This observation suggests that, for phage utilizing SAR-endolysins, the holin controls the time of host lysis due to its ability to trigger and permeabilize the cytoplasmic membrane at a time dictated by its primary structure. This event would facilitate the instantaneous and quantitative release of the SAR-endolysin from the membrane bringing about abrupt lysis of the host.

Many holin genes encode two proteins due to the presence of a "dual-start" motif at their 5' ends. For the well-studied holin from bacteriophage λ, the shorter product, S105, is the holin. The longer product, S107, antagonizes S105 function and is known

as an antiholin. S105 and S107 are topological isomers which differ in that S105 has an additional transmembrane domain. In S107, the residues that make up this transmembrane domain reside in the cytoplasm. At the time of host lysis, S107 undergoes a topological isomerization due to insertion of its cytoplasmically disposed N-terminus into the membrane. This new isomer has the same topology as S105 and, in fact, functions as a holin.

The holin gene of bacteriophage 21 also encodes two proteins, the holin $S^{21}68$ and the antiholin, $S^{21}71$. Both proteins have two potential transmembrane domains which are connected by a predicted periplasmic loop. Because of this, the potential transmembrane domains of S^{21} can only exist as membrane-inserted or periplasmic forms. Since neither transmembrane domain could reside in the cytoplasm, the relationship that existed for the S105/S107 pair was not possible for $S^{21}68$/ $S^{21}71$. It appeared that the only way for the $S^{21}68$/ $S^{21}71$ pair to be topological isomers was if one of them had a transmembrane domain that exited the membrane and entered the periplasm. Until the discovery of the SAR domain, such an event would be unprecedented, particularly for a polytopic membrane protein.

Inspection of the predicted N-terminal transmembrane domain (TMD1) of S^{21} showed that it was compositionally similar to the established SAR domains of the SAR-endolysin family. These domains typically consist of stretches of 15-25 uncharged residues which are enriched for residues that are weakly hydrophobic. The possibility that TMD1 was a SAR domain that was initially membrane-inserted but then exited the membrane lead to the hypothesis that the only the C-terminal transmembrane domain

(TMD2) of S^{21} necessary for hole formation. This was confirmed by demonstrating that the deletion of the sequence encoding TMD1 from *$S^{21}68$* did not abolish its lethality, but only affected the timing of the lethal event. Next, a combination of disulfide crosslinking and protease shaving experiments demonstrated that TMD1 of $S^{21}68$ was initially membrane-inserted but later left the membrane and entered the periplasm and that the kinetics of this process was correlated with hole formation.

Further experiments have indicated that TMD1 has an important role in the regulation of hole formation by TMD2. When TMD1 is "locked" in the membrane by the addition of positively charged residues to the N-terminus of $S^{21}68$, hole formation was blocked. Moreover, this derivative of $S^{21}68$ was able to inhibit hole formation when co-expressed with wild type $S^{21}68$. A preliminary mutational analysis of $S^{21}68$ has provided additional evidence supporting our contention that both heterotypic and homotypic interactions between the two TMDs of S^{21} are important in hole formation and its timing.

The best studied phage endolysins are the R transglycosylase of λ and the E N-acetylmuramidase of T4. Both are soluble, cytoplasmic proteins which must pass through the cytoplasmic membrane in their native conformation in order to gain access to their substrate, peptidoglycan, which resides in the periplasm. As a consequence, the holins of both λ and T4 make relatively large lesions in the cytoplasmic membranes of their hosts. In fact, the hole made by S^{λ} allows the passage of molecules with masses in excess of 500kDa, much larger than is necessary for the escape of the its cognate transglycolsylase. The holins of bacteriophage encoding SAR endolysins need not make

holes large enough to permit the passage of small proteins. In fact, to fulfill their role in controlling the timing of lysis, these holins need only depolarize the membrane which can be accomplished by allowing the free movement of protons. Thus, it was conceivable that S^{21} made holes much smaller than those made by S^{λ}. To explore this possibility we took advantage of a GFP fusion protein that is exported to the periplasm. Cells were allowed to accumulate the fluorescent protein in the periplasmic compartment prior to the induction of either the S^{λ} or S^{21} holin genes. Induction of S^{λ} resulted in the diffusion of the fluorescent protein across the membrane into the cytoplasm while induction of S^{21} had no effect on its distribution. Thus, the holes formed by S^{21} are considerably smaller than those formed by S^{λ}. Thus, to fulfill their role in controlling the timing of lysis, holins for phage with SAR endolysins need only depolarize the membrane; forming large membrane lesions, as has been shown with S^{λ}, would not be necessary. This raises the possibility that holins serving SAR endolysins may not function with canonical, soluble endolysins to effect saltatory host lysis.

REFERENCES

Abedon,S.T. (2006) Phage Ecology. In *The Bacteriophages*. Calendar,R. (ed). New York: Oxford University Press, pp. 37-46.

Barenboim,M., Chang,C.Y., Dib,H.F., and Young,R. (1999) Characterization of the dual start motif of a class II holin gene. *Mol Microbiol* **32**: 715-727.

Bienkowska-Szewczyk,K., Lipinska,B., and Taylor,A. (1981) The R gene product of bacteriophage lambda is the murein transglycosylase. *Mol Gen Genet* **184**: 111-114.

Black,L.W. and Hogness,D.S. (1969) The lysozyme of bacteriophage lambda. I. Purification and molecular weight. *J Biol Chem* **244**: 1968-1975.

Bläsi,U., Chang,C.Y., Zagotta,M.T., Nam,K.B., and Young,R. (1990) The lethal lambda S gene encodes its own inhibitor. *EMBO J* **9**: 981-989.

Bläsi,U., Nam,K., Hartz,D., Gold,L., and Young,R. (1989) Dual translational initiation sites control function of the lambda S gene. *EMBO J* **8**: 3501-3510.

Bonovich,M.T., Young,R. (1991) Dual start motif in two lambdoid S genes unrelated to lambda S. *J Bacteriol* **173**: 2897-2905.

Casjens,S., Eppler,K., Parr,R., and Poteete,A.R. (1989) Nucleotide sequence of the bacteriophage P22 gene 19 to 3 region: identification of a new gene required for lysis. *Virology* **171**: 588-598.

Chang,C.Y., Nam,K., Bläsi,U., and Young,R. (1993) Synthesis of two bacteriophage lambda S proteins in an *in vivo* system. *Gene* **133**: 9-16.

Chang,C.Y., Nam,K., and Young,R. (1995) S gene expression and the timing of lysis by bacteriophage lambda. *J Bacteriol* **177**: 3283-3294.

Cheng,X., Zhang,X., Pflugrath,J.W., and Studier,F.W. (1994) The structure of bacteriophage T7 lysozyme, a zinc amidase and an inhibitor of T7 RNA polymerase. *Proc Natl Acad Sci USA* **91**: 4034-4038.

Deaton,J., Savva,C.G., Sun,J., Holzenburg,A., Berry,J., and Young,R. (2004) Solubilization and delivery by GroEL of megadalton complexes of the lambda holin. *Protein Sci* **13**: 1778-1786.

Deber,C.M., Liu,L.P., and Wang,C. (1999) Perspective: peptides as mimics of transmembrane segments in proteins. *J Pept Res* **54**: 200-205.

DeLisa,M.P., Samuelson,P., Palmer,T., and Georgiou,G. (2002) Genetic analysis of the twin arginine translocator secretion pathway in bacteria. *J Biol Chem* **277**: 29825-29831.

Doermann,A.H. (1948) Lysis and lysis inhibition with *Escherichia coli* Bacteriophage. *J Bacteriol* **55**: 257-276.

Evrard,C., Fastrez,J., and Declercq,J.P. (1998) Crystal structure of the lysozyme from bacteriophage lambda and its relationship with V and C-type lysozymes. *J Mol Biol* **276**: 151-164.

Fuhrman,J.A. (1999) Marine viruses and their biogeochemical and ecological effects. *Nature* **399**: 541-548.

Garrett,J.M. and Young,R. (1982) Lethal action of bacteriophage lambda S gene. *J Virol* **44**: 886-892.

Goldberg,A.R., Howe,M. (1969) New mutations in the S cistron of bacteriophage lambda affecting host cell lysis. *Virology* **38**: 200-202.

Graschopf,A., Bläsi,U. (1999a) Functional assembly of the lambda S holin requires periplasmic localization of its N-terminus. *Arch Microbiol* **172**: 31-39.

Graschopf,A., Bläsi,U. (1999b) Molecular function of the dual-start motif in the λ S holin. *Mol Microbiol* **33**: 569-582.

Greene,E.A., Codomo,C.A., Taylor,N.E., Henikoff,J.G., Till,B.J., Reynolds,S.H., Enns,L.C., Burtner,C., Johnson,J.E., Odden,A.R., Comai,L., and Henikoff,S. (2003) Spectrum of chemically induced mutations from a large-scale reverse-genetic screen in *Arabidopsis*. *Genetics* **164**: 731-740.

Gründling,A., Bläsi,U., and Young,R. (2000a) Biochemical and genetic evidence for three transmembrane domains in the class I holin, lambda S. *J Biol Chem* **275**: 769-776.

Gründling,A., Bläsi,U., and Young,R. (2000b) Genetic and biochemical analysis of dimer and oligomer interactions of the lambda S holin. *J Bacteriol* **182**: 6082-6090.

Gründling,A., Manson,M.D., and Young,R. (2001) Holins kill without warning. *Proc Natl Acad Sci USA* **98**: 9348-9352.

Gründling,A., Smith,D.L., Bläsi,U., and Young,R. (2000c) Dimerization between the holin and holin inhibitor of phage lambda. *J Bacteriol* **182**: 6075-6081.

Guyer,M.S., Reed,R.R., Steitz,J.A., and Low,K.B. (1981) Identification of a sex-factor-affinity site in *E. coli* as gamma delta 6. *Cold Spring Harb Symp Quant Biol* **45 Pt 1**: 135-140.

Hanych,B., Kedzierska,S., Walderich,B., Uznanski,B., and Taylor,A. (1993) Expression of the Rz gene and the overlapping Rz1 reading frame present at the right end of the bacteriophage lambda genome. *Gene* **129**: 1-8.

Hendrix,R.W., Smith,M.C., Burns,R.N., Ford,M.E., and Hatfull,G.F. (1999) Evolutionary relationships among diverse bacteriophages and prophages: all the world's a phage. *Proc Natl Acad Sci USA* **96**: 2192-2197.

Hershey,A.D. (1946) Spontaneous mutations in bacterial viruses. In *Heredity and Variation in Microorganisms*. Cold Spring Harbor, L.I., N.Y.: Cold Spring Harbor Symposia on Quantitative Biology, pp. 67-77.

Inouye,H., Barnes,W., and Beckwith,J. (1982) Signal sequence of alkaline phosphatase of *Escherichia coli*. *J Bacteriol* **149**: 434-439.

Inouye,M., Arnheim,N., and Sternglanz,R. (1973) Bacteriophage T7 lysozyme is an N-acetylmuramyl-L-alanine amidase. *J Biol Chem* **248**: 7247-7252.

Jacob,F., Fuerst,C.R. (1958) The mechanism of lysis by phage studied with defective lysogenic bacteria. *J Gen Microbiol* **18**: 518-526.

Javadpour,M.M., Eilers,M., Groesbeek,M., and Smith,S.O. (1999) Helix packing in polytopic membrane proteins: role of glycine in transmembrane helix association. *Biophys J* **77**: 1609-1618.

Kiino,D.R., Silhavy,T.J. (1984) Mutation prlF1 relieves the lethality associated with export of beta-galactosidase hybrid proteins in *Escherichia coli*. *J Bacteriol* **158**: 878-883.

Kolisnychenko,V., Plunkett,G., III, Herring,C.D., Feher,T., Posfai,J., Blattner,F.R., and Posfai,G. (2002) Engineering a reduced *Escherichia coli* genome. *Genome Res* **12**: 640-647.

Lemmon,M.A., Flanagan,J.M., Hunt,J.F., Adair,B.D., Bormann,B.J., Dempsey,C.E., and Engelman,D.M. (1992) Glycophorin A dimerization is driven by specific interactions between transmembrane alpha-helices. *J Biol Chem* **267**: 7683-7689.

Loessner,M.J., Wendlinger,G., and Scherer,S. (1995) Heterogeneous endolysins in *Listeria monocytogenes* bacteriophages: a new class of enzymes and evidence of conserved holin genes within the siphoviral lysis cassettes. *Mol Microbiol* **16**: 1231-1241.

Lwoff,A., Horne,R., and Tournier,P. (1962) A system of viruses. *Cold Spring Harb Symp Quant Biol* **27**.

MacKenzie,K.R., Engelman,D.M. (1998) Structure-based prediction of the stability of transmembrane helix-helix interactions: the sequence dependence of glycophorin A dimerization. *Proc Natl Acad Sci USA* **95**: 3583-3590.

Miller,J.H. (1992) Mutagenesis with EMS. Plain View, New York: Cold Spring Harbor Laboratory Press, pp. 135-142.

Ozaki,M., Valentine,R.C. (1973) Inhibition of bacterial cell wall mucopeptide synthesis: a new function of RNA bacteriophage Qbeta. *Biochim Biophys Acta* **304**: 707-714.

Park,T., Struck,D.K., John,F.D., and Young,R. (2007) Topological dynamics of holins in programmed bacterial lysis. *Proc Natl Acad Sci USA* accepted.

Raab,R., Neal,G., Garrett,J., Grimaila,R., Fusselman,R., and Young,R. (1986) Mutational analysis of bacteriophage lambda lysis gene S. *J Bacteriol* **167**: 1035-1042.

Raab,R., Neal,G., Sohaskey,C., Smith,J., and Young,R. (1988) Dominance in lambda S mutations and evidence for translational control. *J Mol Biol* **199**: 95-105.

Ramanculov,E. and Young,R. (2001a) Functional analysis of the phage T4 holin in a lambda context. *Mol Genet Genomics* **265**: 345-353.

Ramanculov,E. and Young,R. (2001b) Genetic analysis of the T4 holin: timing and topology. *Gene* **265**: 25-36.

Rennell,D. and Poteete,A.R. (1985) Phage P22 lysis genes: nucleotide sequences and functional relationships with T4 and λ genes. *Virol* **143**: 280-289.

Rietsch,A., Fraisl,P., Graschopf,A., and Bläsi,U. (1997) The hydrophilic C-terminal part of the lambda S holin is non-essential for intermolecular interactions. *FEMS Microbiol Let* **153**: 393-398.

Rydman,P.S. and Bamford,D.H. (2003) Identification and mutational analysis of bacteriophage PRD1 holin protein P35. *J Bacteriol* **185**: 3795-3803.

Sao-Jose,C., Parreira,R., Vieira,G., and Santos,M.A. (2000) The N-terminal region of the Oenococcus oeni bacteriophage fOg44 lysin behaves as a bona fide signal peptide in Escherichia coli and as a cis-inhibitory element, preventing lytic activity on oenococcal cells. *J Bacteriol* **182**: 5823-5831.

Schagger,H., von,J.G. (1987) Tricine-sodium dodecyl sulfate-polyacrylamide gel electrophoresis for the separation of proteins in the range from 1 to 100 kDa. *Anal Biochem* **166**: 368-379.

Senes,A., Engel,D.E., and DeGrado,W.F. (2004) Folding of helical membrane proteins: the role of polar, GxxxG-like and proline motifs. *Curr Opin Struct Biol* **14**: 465-479.

Senes,A., Gerstein,M., and Engelman,D.M. (2000) Statistical analysis of amino acid patterns in transmembrane helices: the GxxxG motif occurs frequently and in association with beta-branched residues at neighboring positions. *J Mol Biol* **296**: 921-936.

Senes,A., Ubarretxena-Belandia,I., and Engelman,D.M. (2001) The Calpha ---H...O hydrogen bond: a determinant of stability and specificity in transmembrane helix interactions. *Proc Natl Acad Sci USA* **98**: 9056-9061.

Smith,D.L., Chang,C.Y., and Young,R. (1998a) The λ holin accumulates beyond the lethal triggering concentration under hyperexpression conditions. *Gene Expr* **7**: 39-52.

Smith,D.L., Struck,D.K., Scholtz,J.M., and Young,R. (1998b) Purification and biochemical characterization of the lambda holin. *J Bacteriol* **180**: 2531-2540.

Smith,D.L., Young,R. (1998c) Oligohistidine tag mutagenesis of the lambda holin gene. *J Bacteriol* **180**: 4199-4211.

Sonnhammer,E.L., von Heijne,G., and Krogh,A. (1998) A hidden Markov model for predicting transmembrane helices in protein sequences. *Proc of Sixth Int Conf on Intelligent Systems for Molecular Biology* **6**: 175-182.

Streisinger,G., Mukai,F., Dreyer,W.J., Miller,B., and Horiuchi,S. (1961) Mutations affecting the lysozyme of phage T4. *Cold Spring Harb Symp Quant Biol* **26**: 25-30.

Summer, E. J. and Young, R. Unpublished Work. Practical genomics for undergraduates, Texas A&M University. 2006.

Taylor,A. (1971) Endopeptidase activity of phage λ-endolysin. *Nature New Biol* **234**: 144-145.

Tran,T.A., Struck,D.K., and Young,R. (2005) Periplasmic domains define holin-antiholin interactions in t4 lysis inhibition. *J Bacteriol* **187**: 6631-6640.

Tsugita,A., Inouye,M. (1968a) Complete primary structure of phage lysozyme from *Escherichia coli* T4. *J Mol Biol* **37**: 201-212.

Tsugita,A., Inouye,M. (1968b) Purification of bacteriophage T4 lysozyme 7. *J Biol Chem* **243**: 391-397.

Van Regenmortel, M. (2000) Virus Taxanomy. San Diego, California, Academic Press. Seventh Report of the International Committee on Taxanomy of Viruses.

Vilen,H., Aalto,J.M., Kassinen,A., Paulin,L., and Savilahti,H. (2003) A direct transposon insertion tool for modification and functional analysis of viral genomes. *J Virol* **77**: 123-134.

von Heijne,G. (1989) Control of topology and mode of assembly of a polytopic membrane protein by positively charged residues. *Nature* **341**: 456-458.

Wang,I.N., Deaton,J., and Young,R. (2003) Sizing the holin lesion with an endolysin-beta-galactosidase fusion. *J Bacteriol* **185**: 779-787.

Wang,I.N., Dykhuizen,D.E., and Slobodkin,L.B. (1996) The evolution of phage lysis timing. *Evol Ecol* **10**: 545-558.

Wang,I.N., Smith,D.L., and Young,R. (2000) Holins: the protein clocks of bacteriophage infections. *Annu Rev Microbiol* **54**: 799-825.

Weaver,L.H., Matthews,B.W. (1987) Structure of bacteriophage T4 lysozyme refined at 1.7 A resolution. *J Mol Biol* **193**: 189-199.

Wheeler,D.L., Chappey,C., Lash,A.E., Leipe,D.D., Madden,T.L., Schuler,G.D., Tatusova,T.A., and Rapp,B.A. (2000) Database resources of the National Center for Biotechnology Information. *Nucleic Acids Res* **28**: 10-14.

Wimley,W.C., White,S.H. (2000) Designing transmembrane alpha-helices that insert spontaneously. *Biochemistry* **39**: 4432-4442.

Work,E. (1967) Factors affecting the susceptibility of bacterial cell walls to the action of lysozyme. *Proc R Soc Lond B Biol Sci* **167**: 446-447.

Xu,M., Arulandu,A., Struck,D.K., Swanson,S., Sacchettini,J.C., and Young,R. (2005) Disulfide isomerization after membrane release of its SAR domain activates P1 lysozyme. *Science* **307**: 113-117.

Xu,M., Struck,D.K., Deaton,J., Wang,I.N., and Young,R. (2004) A signal-arrest-release sequence mediates export and control of the phage P1 endolysin. *Proc Natl Acad Sci USA* **101**: 6415-6420.

Young,R. (1992) Bacteriophage lysis: mechanism and regulation. *Microbiol Rev* **56**: 430-481.

Young,R. (2002) Bacteriophage holins: deadly diversity. *J Mol Microbiol Biotechnol* **4**: 21-36.

Young,R. and Bläsi,U. (1995) Holins: form and function in bacteriophage lysis. *FEMS Microbiol Rev* **17**: 191-205.

Young,R., Wang,I.N., and Roof,W.D. (2000) Phages will out: strategies of host cell lysis. *Trends Microbiol* **8**: 120-128.

Young,R., Way,J., Way,S., Yin,J., and Syvanen,M. (1979) Transposition mutagenesis of bacteriophage lambda: a new gene affecting cell lysis. *J Mol Biol* **132**: 307-322.

Zhang,N., Young,R. (1999) Complementation and characterization of the nested Rz and Rz1 reading frames in the genome of bacteriophage lambda. *Mol Gen Genet* **262**: 659-667.

VITA

Name: Taehyun Park

Address: Biochemistry and Biophysics, Room 315, MS 2128, Texas A&M University, College Station, TX 77843-2128

Email Address: parkt@yahoo.com

Education: B.A., Genetic Engineering, Kyungpook National University, Taegu, Republic of Korea, 1994
M.S., Biological Sciences, Minnesota State University, Mankato, MN, 1999
Ph.D., Biochemistry and Biophysics, Texas A&M University, College Station, TX, 2006